Influence of covariance of aerosol and meteorology on co-located precipitating and non-precipitating clouds over Indo-Gangetic Plains

Nabia Gulistan[1], Khan Alam[1*], Yangang Liu[2]

[1]Department of Physics, University of Peshawar, Peshawar, 25120, Pakistan

[2]Environmental & Climate Science Department, Brookhaven National Laboratory, USA

Correspondence: Khan Alam (khanalam@uop.edu.pk)

HIGHLIGHTS

- Strong aerosol-cloud relation under unstable meteorological conditions led to formation of high-level thick clouds.
- In thick clouds the activation of cloud droplets is weakly dependent on aerosols.
- Optically thin clouds led to high precipitation rate.

ABSTRACT

Aerosol-cloud-precipitation-interaction (ACPI) plays a pivotal role in the global and regional water cycle and the earth's energy budget; however, it remains highly uncertain due to the underlying different physical mechanisms. Therefore, this study aims to systematically analyze the effects of aerosols and meteorological factors on ACPI in the co-located precipitating (PCs) and non-precipitating clouds (NPCs) clouds in winter and summer seasons by employing the long-term (2001-2021) retrievals from Moderate Resolution Imaging Spectroradiometer (MODIS), Tropical Rainfall Measuring Mission (TRMM), and National Center for Environmental Prediction/National Center for Atmospheric Research (NCEP/NCAR) reanalysis-II datasets over the Indo-Gangetic Plains (IGP). The results exhibit a decadal increase in aerosol optical depth (AOD) over Lahore (5.2%), Delhi (9%), Kanpur (10.7%) and Gandhi College (22.7%) and decrease over Karachi (-1.9%) and Jaipur (-0.5%). The most stable meteorology with high values of lower tropospheric stability (LTS) is found in both seasons over Karachi. In summer season the occurrence frequency of clouds is high (74%) over Gandhi College, 60% of which are PCs. Conversely, the least number of PCs are found over Karachi. Similarly, in winter season, the frequency of cloud occurrence is low over Karachi and high over Lahore and Gandhi College. The analysis of cloud top pressure (CTP) and cloud optical thickness (COT) indicate high values of cloud fraction (CF) for thick and high-level clouds over all study areas except Karachi. The micro-physical properties such as cloud effective radius (CER) and cloud droplet number concentration (CDNC) bears high values (CER

$> \sim 15$ μm and CDNC $> \sim 50$ cm^{-3}) for both NPCs and PCs in summer. The AOD-CER correlation is good (weak) for PCs (NPCs) in winter. Similarly, the sensitivity value of the first indirect effect (FIE) is high (ranged from 0.2 ± 0.13 to 0.3 ± 0.01 in winter, and from 0.19 ± 0.03 to 0.32 ± 0.05 in summer) for PCs and low for NPCs. Sensitivity value for second indirect effect (SIE) is relatively high (such as 0.6 ± 0.14 in winters and 0.4 ± 0.04 in summer) than FIE. Sensitivity values of the aerosol-cloud interaction (ACI) are low (i.e., -0.06 ± 0.09) for PCs in summers. Furthermore, the precipitation rate (PR) exhibits high values in summer season, and PR values are found high in comparatively thin clouds with fewer CDNC ($< \sim 50$ cm^{-3}) and intermediate for optically thick clouds with higher CDNC ($> \sim 50$ cm^{-3}).

Keywords: Aerosol-cloud-precipitation-interaction, Aerosol optical depth, cloud effective radius, cloud droplet number concentration, lower tropospheric stability, relative humidity, first indirect effect, second indirect effect, precipitation sensitivity.

1. Introduction

The aerosol-cloud-precipitation-interaction (ACPI) and aerosol-radiation-interaction (ARI) significantly influence climates at the regional and global scales (Romero et al., 2021). Assessing the direct and indirect effects of aerosols is crucial to understand and predict energy budget and the water cycle. In the direct effect, the absorption and scattering of solar radiation by aerosols lead to the warming of the atmosphere and cooling of the earth's surface (Zhou et al., 2020), causing changes in the lower tropospheric stability (LTS) that further leads to modulation of precipitating (PCs) and non-precipitation clouds (NPCs) (Andreae & Rosenfeld, 2008). In the indirect effect, the water-soluble aerosols such as soil dust, sulfates, nitrates, and other organic aerosols ejected naturally and anthropogenically serve as cloud condensation nuclei (CCN) and ice nucleating particle (INP). Hence, aerosols affect the aerosol-cloud-interaction (ACI) by influencing the growth of cloud droplet and cloud droplet number concentration (CDNC) (Twomey et al., 1977; Albrecht, 1989; Jiang et al., 2002; Chen et al., 2011; Tao et al., 2012). The increase of CDNC and decrease of cloud droplet effective radius (CER) inhibit the onset of precipitation and increase the cloud lifetime (Albrecht, 1989). Conversely, the decrease in CDNC and increase in CER increases the probability of precipitation rate (PR). Conversely, Stevens and Feingold (2009) have shown that initially, more sea salt carried by high wind speed inhibit the

61 precipitation formation. However, the same sea spray tends to seed the coalescence by producing

62 larger CER that led to enhanced precipitation.

63 In the last few decades, most of the cultivable land of the Indo-Gangetic Plain (IGP) has been

64 replaced by urban developments. Due to the fastest growth of population, urbanization,

65 industrialization, and massive combustion of biomass and fossil fuels in residential homes and

66 factories, a decadal increase in aerosols is observed over IGP. The high aerosol loading may affect

67 the formation of tropospheric clouds and seasonal precipitation patterns (Kaskaoutis et al., 2011;

68 Singh et al., 2015; Thomas et al., 2021) and makes IGP suitable for the study of ACPI. Besides,

69 frequent variations in cloud fraction (CF), extreme precipitation and drought abrupt temperature

70 changes (e.g., heat waves), and irregular unseasonal rains may cause major and unavoidable

71 hazards at local and regional levels in the future.

72 In the last two decades, the scientific community has focused on quantification of ACI using both

73 observations (Feingold et al., 2003; Costantino et al., 2010; Zhao et al., 2018, 2020; Anwar et al.,

74 2022) and modeling techniques (Chen et al., 2016, 2018; Wang et al. 2020; Zhou et al., 2020;

75 Sharma et al., 2023). Although, a similar recent study (Anwar et al., 2022) attempted to understand

76 the sensitivities of ACI and the first indirect effect of different subsets of AOD to the different

77 conditions of RH and wind directions and found decrease (increase) in CER with aerosol loading

78 Twomey effect (anti-Twomey effect) over the monsoon (weak and moderately intensive monsoon)

79 regions. However, the above study excluded the other significant meteorological parameters such

80 as LTS, PR, and T_{850} and was also limited to the monsoon regions of Pakistan only. Further, in the

81 context of warm rain processes, it is generally understood that the high concentration of aerosols

82 capable of serving as CCN leads to enhanced CDNC known as the first indirect effect (FIE) or

83 Twomey effect (Twomey et al., 1977). It is also widely acknowledged that CDNC plays a pivotal

84 role in cloud microphysics and significantly influences the onset of precipitation and retention of

85 water in clouds called the second indirect effect (SIE) (Gryspeerdt et al., 2016; Naud et al., 2017).

86 Whilst, in the above study, the analysis of CDNC is also not addressed. Therefore, the present

87 study aims to deepen the previous study (Anwar et al., 2022), by a long-term and detailed analysis

88 of the ACPI including aerosol-indirect effects for low-level clouds extended over the whole IGP

89 for understanding different mechanisms (condensation, droplet growth and precipitation rate) of

90 cloud and precipitation formation.

91 This study is focused on estimating the variations in sensitivities of aerosol-cloud relationship to
92 the variations in aerosol loading at specified meteorological conditions for low-level PCs and
93 NPCs in the summer and winter seasons over the IGP. This study is unique in using a large number
94 of samples, classification of liquid clouds in PCs and NPCs, further classification of clouds in low,
95 mid, and high-level clouds through joint COT-CTP histograms, quantification of the sensitivities
96 of FIE, SIE, total indirect effect (TIE), and ACI to CDNC. The significant meteorological
97 parameters considered include temperature at 850 hPa, LTS, relative humidity (RH%) at 850 hPa,
98 vertical velocity (Ω), and PR. Furthermore, by utilizing the Moderate Resolution Imaging
99 Spectroradiometer (MODIS) and Tropical Rainfall Measuring Mission (TRMM) data, the
100 correlation of cloud microphysical properties (CER and CDNC) and AOD at specified values of
101 LTS and cloud liquid water path (CLWP) is examined, and precipitation sensitivity at constant
102 macro-physical condition is estimated.

103 **2. Study area and methodology**

104 2.1. Study area

105 The selected study area (Fig. 1) comprises the upper, middle, and eastern portions of the IGP. The
106 upper part consists of the densely populated and developed regions of the eastern part of Pakistan
107 i.e., Karachi (24.87ºN, 67.03ºE) and Lahore (31.54ºN, 74.32ºE) whereas the middle part comprises
108 the northern part of India i.e., Delhi (28.59ºN, 77.22ºE), Kanpur (26.51ºN, 80.23ºE), Jaipur
109 (26.91ºN, 75.81ºE), Gandhi College (25.87ºN, 84.13ºE), Kolkata (22.57ºN, 88.36ºE), Dhaka
110 (23.80ºN, 90.41ºE) and Patna (25.59ºN, 85.13ºE). The data analysis for the eastern part of IGP
111 (Kolkata, Dhaka and Patna) is documented as supplementary materials.

112
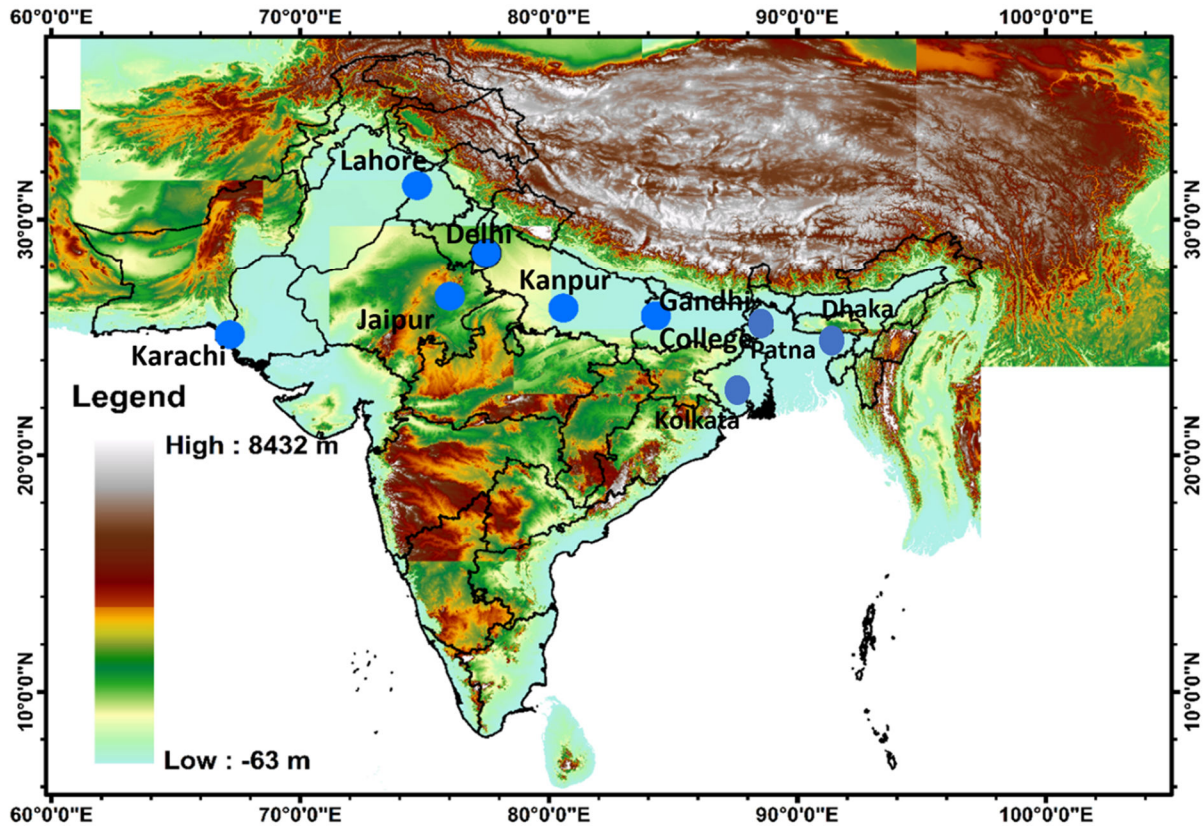
113 **Figure 1.** Topography of the study area.

114 **2.2. Methodology**

115 2.2.1. MODIS, NCEP/NCAR reanalysis-II and TRMM data

116 Moderate Resolution Imaging Spectroradiometer (MODIS) is a major constituent of NASA's Earth

117 Observing System (EOS). MODIS is orbiting with two onboard satellites, Terra and Aqua,

118 launched in 1999 and 2002 respectively, with a range of 2330 km spanning the entire globe in a

119 day. It provides data and information with a spatial resolution of 1° to study atmospheric processes

120 and physical structure (Kedia et al., 2014; Srivastava et al., 2015). This study uses the daily mean

121 of combined dark target and deep blue AOD at 0.55 µm, cloud top pressure (CTP), cloud top

122 temperature (CTT), CF, CER, and COT for liquid clouds from level 3 aerosol-cloud data product

123 MOD08-TERRA. Data with AOD > 1.5 are excluded to avoid potential misidentification of

124 aerosols as clouds . The following adiabatic approximation (Brenguier et al., 2000; Wood, 2006;

125 Kubar et al., 2009; Michibata et al., 2014) is used to calculate CDNC (cm^{-3}):

$$\text{CDNC} = \left(\frac{B}{\text{CER}}\right)^3 * \sqrt{(2 * \text{CLWP} * \gamma_{\text{eff}})}$$

126

127
(1)

128 Where $B = \sqrt[3]{\left(\frac{3}{4}\pi\rho_{water}\right)}$ =0.0620, ρ_{water} is the liquid water density, γ_{eff} is the adiabatic

129 gradient of liquid water content in the moist air column (Wood, 2006). Value of γ_{eff} range from 1

130 to 2.5×10^{-3} at a temperature of 32 K to 104 K (Brenguier, 1991; Zhu et al., 2018; Zhou et al.,

131 2020). The CLWP is estimated by use of

$$CLWP = \frac{5\rho_w(CER)(COT)_w}{9},$$

132

133
(2)

134 Where, ρ_w is the water density at room temperature (Koike et al., 2016).

135 National Center for Environmental Prediction/National Center for Atmospheric Research

136 (NCEP/NCAR) reanalysis datasets provide global reanalysis data sets that combine satellite

137 observations with the simulation of models through data assimilation (Purdy et al., 2016). Daily

138 data for meteorological parameters including temperature, RH%, and Ω at 850 hPa are retrieved

139 at a spatial resolution of T62 Gaussian grid (1.915° × 1.875°) from NCEP reanalysis-II datasets,

140 and used to calculate lower tropospheric stability (LTS) defined as (Li et al., 2017):

$$LTS = \theta_{700} - \theta_{1000}$$

141
(3)

142

143 where θ is the potential temperature and the subscripts denote the pressure levels of 700
144 hPa and1000 hPa.

145 The Tropical Rainfall Measuring Mission (TRMM) is the first Joint satellite mission between

146 NASA America and National Space Development Agency (NASDA) Japan, utilizing the visible

147 infrared and microwaves to measure the rain precipitation over tropical and subtropical regions.

148 The main TRMM instruments that are used to measure rain precipitation are precipitation radar

149 (PR) and TRMM Microwave Imager (TMI). Where PR is operating at a frequency of 13.8 GHz

150 and TMI is a passive microwave radiometer consisting of nine channels. A calibrated data set

151 TRMM-2B31 of TRMM Combined Instrument (TCI) for TRMM Multi-Satellite Precipitation

152 Analysis (TMPA) is formed from an algorithm that uses TMI and PR. The product TMPA 3B42

153 gives the rain precipitation averages on a daily and sub-daily basis. In the current study, the data
154 product TMPA or TRMM 3B42 is used for the retrieval of PR on daily basis. The spatial resolution
155 of TRMM 3B42 is 0.25º × 0.25º and is available from the year 1998 to till date.

156 ### 2.2.2. Methodology

157 The present study is designed to analyze and quantify the ACPI for PCs and NPCs in winter and
158 summer under a variety of meteorological conditions. The daily mean data of each parameter for
159 warm clouds are retrieved from the respective satellites and NCEP/NCAR reanalysis-II for each
160 study site. Subsequently, in this analysis, the VLOOKUP function is utilized for linear
161 interpolation/alignment of the data. This function is available as a built-in feature in Microsoft
162 Excel. The data are then segregated into two subsets for the summer and winter seasons. Based on
163 precipitation data from TRMM, the subsets are further divided into precipitating and non-
164 precipitating clouds.

165 The sensitivities of cloud parameters to CDNC are analyzed through the following formulation
166 considered from previous studies (Zhou et al., 2020):

167
$$\frac{dln(COT)}{dln(CDNC)} = -\frac{dln(CER)}{dln(CDNC)} + \frac{dln(CLWP)}{dln(CDNC)} \qquad (4)$$

168 In this study, the term on the left side of equation (3) is defined as total indirect aerosol effect
169 (TIE), and the first and second terms on the right side of the equation are defined as the first indirect
170 aerosol effect (FIE), $and\ second\ indirect\ effect\ (SIE), respectively$. Similarly, the sensitivity
171 of CDNC to AOD is evaluated by employing the index of ACI:

172
$$\mathrm{ACI_{CDNC}} = \frac{dln(CDNC)}{dln(AOD)} \qquad (5)$$

173 The sensitivity of PR to CDNC is calculated from the following equation (Jung et al., 2012) :

174
$$\mathrm{S_0} = \left(-\frac{\partial ln(PR)}{\partial ln\ (CDNC)}\right)_{COT} \qquad (6)$$

3. Results and Discussion

3.1. Regional and seasonal distribution of AOD

AOD is a commonly used proxy for aerosol concentration in the atmosphere and is analyzed here (Fig. 2-3).

IGP characteristically exhibits a diverse and massive pool of aerosols due to its unique topography. The western part of IGP is a coastal location and inlet for the westerly winds. Therefore, dry regions and Arabian sea in the west contribute dust, sea salt and water vapors to the region. The Himalayas in the north act as barriers to the winds, leading to the trapping of aerosols over the central part of IGP. Therefore, this region exhibits a high concentration of anthropogenic aerosols. Bay of Bengal in the east allows southeasterly winds to enter passing across Dhaka, Kolkata, Patna to Delhi and Lahore (Hassan et al., 2002; Anwar et al., 2022). The westerly and easterly winds traverse forested hilly terrain, rivers and lakes elevating humidity level and initiate the cloud formation by activation of the newly originated small aerosol particles as CCNs and cloud formation affecting the local microclimate.

Fig. 2 shows a decadal variation in time average maps for combined dark target and deep blue AOD retrieved at 0.55 µm over the entire study area for the years (2001-2010) and (2011-2021). Also, Table 1 illustrates the percentage change in decadal averaged values of AOD. The results indicate that AOD exhibits a decrease over Karachi (-1.9%) and Jaipur (-0.5%). Whilst an increase in AOD is observed over Lahore (5.2%), Delhi (9%), Kanpur (10.7%) and Gandhi College (22.7%). Similarly, Table 1S shows the decadal change in AOD over Kolkata (18%), Dhaka (22.6%) and Patna (23.3%). Similar to Gandhi College, an increase is observed over all the three areas. Reason for the increase of aerosols include multiple sources of aerosols, human behavior, socio-economic development at local and regional level, and unique topography for persistence and retaining of aerosols.

Fig.3(a-b) shows the probability density function (PDF) for AOD, illustrating different distributions in summer and winter season. Fig.3a shows that the distribution of AOD over Delhi, Kanpur, and Gandhi College is similar. However, a shift in peak value of PDF towards high values of AOD over Lahore and low values over Jaipur illustrate comparatively high and low aerosol concentration in summer season over Lahore and Jaipur respectively. Likewise, Fig. 1S shows the

204   seasonal PDF values of AOD over Kolkata, Dhaka and Patna. The results indicate similar seasonal
205   distribution functions over all the three areas of eastern IGP. In both seasons PDF peaks for high
206   values of AOD are observed over Patna showing high concentration of aerosols as compared to
207   Kolkata and Dhaka.

208   The loading of high concentration of aerosols is owing to the high-density of population,
209   industrialization, and human activities. The major sources of aerosols in all months of the year
210   include vehicular emission originated from old transport facilities, emission of smoke and soot
211   during consumption of biomass for cooking, heavy industrial emission, and aerosols produced in
212   seasonal harvesting and crop-reside burning. All these sources produce organic aerosols which are
213   characterized as hydrophilic particles and have the potential to act as CCN. Likewise, the soil dust
214   particles also act as good CCN due to their hydroscopic nature (Sun & Ariya, 2006). Moreover,
215   the meteorological conditions also play a substantial role to enhance AOD values such as the
216   uplifting of loose soil dust and swelling of aerosols due to holding the water vapors (wv) for long
217   time (Masmoudi et al., 2003; Alam et al., 2010; Alam et al., 2011;). Also, the lower but flat PDF
218   curve demonstrates low values of AOD over Karachi. Ali et al., 2020 associated the low AOD
219   values over Karachi to the westerly and southwesterly winds currents at tropospheric level.
220   However, the decreasing trend in AOD over the coastal city may also be attributed to the variations
221   in other meteorological parameters like T and RH.

222   As compared to summer season, the pattern of PDF in winter is significantly different as shown in
223   Fig. 3b. The low value of PDF (0.5) for the high value of AOD (0.9) over Karachi illustrates a
224   comparatively pristine atmosphere. Similarly, the PDF peaks for Lahore, Delhi and Jaipur (0.7, 0.7
225   and 0.8) indicate comparatively high AOD over Delhi. Likewise, the distribution over Kanpur and
226   Gandhi College is similar illustrating similar values of AOD (1.1and 1.2 respectively). These high
227   values of AOD are attributed to the high emission of anthropogenic aerosols at local and regional
228   level over the central part of IGP (Delhi, Jaipur, Kanpur and Gandhi College).

229   Few authors attributed the reduced values of AOD in winter season to the wet scavenging and
230   suppressed emission of aerosols from earth surface (Alam et al., 2010; Zeb et al., 2019). However,
231   in our case, the low (high) values in winter (summer) are associated to dispersion of fine (course)
232   mode particles due to the variations in meteorological conditions.

233
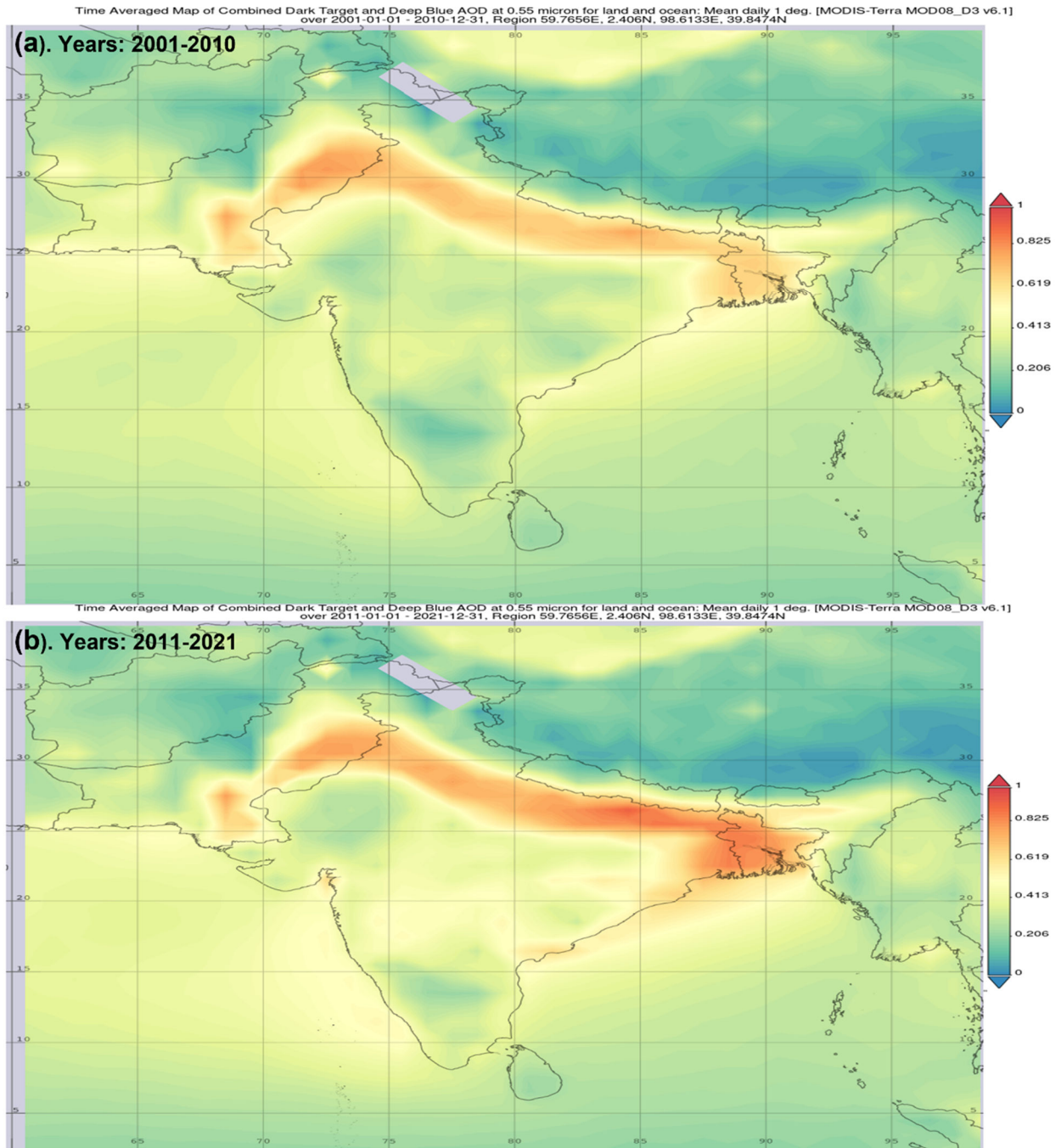
Figure 2. Decadal increase (year: 2001-2010 and 2011-2021) in AOD over study sites.

235

236

237

238

Table 1. Decadal percentage variations in average values of AOD over all study areas

	Karachi	Lahore	Delhi	Kanpur	Jaipur	Gandhi College
Total number of counts	5902	6171	5823	5201	5907	5125
Decadal change in AOD	-1.9%	5.2%	9%	10.7%	-0.5%	22.7%

240

241
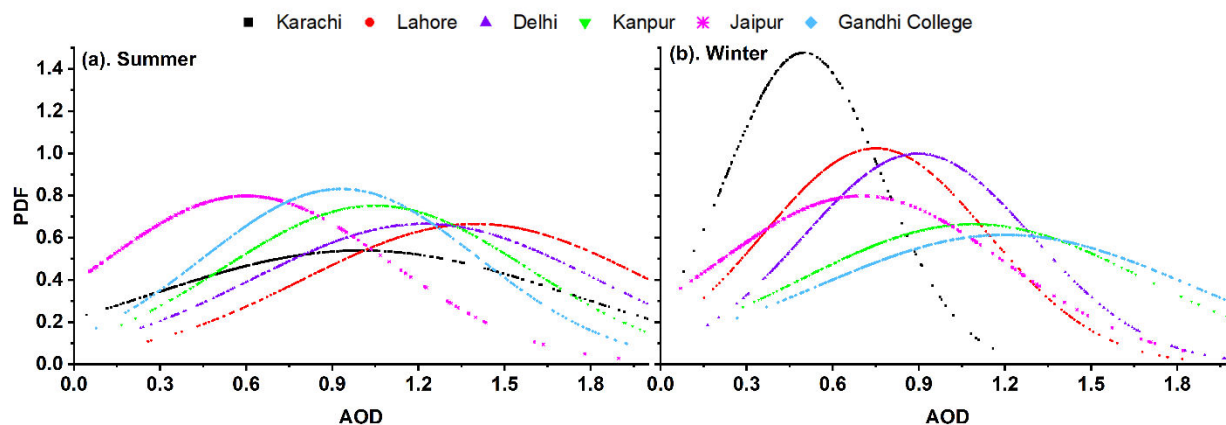
Figure 3. Probability density function (PDF) of AOD over study sites is shown (a) and (b) for summer and winter seasons respectively.

3.2. Climatology of meteorological parameters

Generally, LTS has relationships to factors such as temperature, humidity, wind patterns, and atmospheric pressure over extended periods. It is also widely acknowledged that atmospheric stability, temperature, RH and wind speed and direction play a significant role in cloud formation (Yang et al., 2015; Tao et al., 2012). Therefore, the influence of long-term variations in the said meteorological parameters are considered in the current study. The variations in meteorological parameters have an unavoidable impact on ACPI. The parameters considered in this study include the temperature, LTS to determine the lower atmospheric stability and instability that influence the process of cloud and precipitation formation through its significant implications on evaporation and convection of the air parcel, the RH% to estimate the level of wv and the Ω to assess the suitable atmospheric dynamics. Fig.4 shows the variations in LTS values for NPCs and PCs in winter and summer season. In winter season, the LTS values are high for NPCs and comparatively lower for PCs over entire study areas. In summer season, the scenario is reversed with high values for PCs but low values for NPCs, suggesting stable tropospheric layer on rainy days. This

258 stabilization may be attributed to the cold pools generated by the evaporation of falling rain
259 droplets (Wu et al., 2017). The lower LTS values for NPCs in summer season suggest the
260 likelihood of stronger instability that causes high potential of vertical motion and development of
261 thunderstorm. However, Karachi exhibits a distinct pattern of LTS with the highest values in each
262 case, which indicates the existence of the most stable tropospheric layer in Karachi due likely to
263 moist and cold sea breeze   due to the city's coastal location.

264 The median values computed for the remaining meteorological parameters considered in this study
265 are listed in Table 2. The high values in each case are indicated in bold and low values are italicized.
266 The results show that in winter season the temperature at 850 hPa (T_{850}) is relatively high for NPCs
267 ranging from 281 K to 285.6 K. The increase in RH% for PCs during winter ranged from (59.5)%
268 to (71.5)%. Also, the Ω > 0 for NPCs and < 0 for PCs in winter season.

269 In summer season, it is observed that T_{850} is comparatively higher than that for the winter clouds
270 and ranged from 298.3 to 300.2 K and 296.5 to 298.3 K for NPCs and PCs respectively. The high
271 values of T_{850} are due to intense solar fluxes in summer season that keep the temperature of the
272 earth's surface and adjacent atmospheric layer higher. Also, the increase in RH% during summer
273 ranged between 33.5-51.7 % for NPCs. The reason for the high values of wv and RH% is mainly
274 the suitable thermodynamical conditions such as evaporation and convection due to the high
275 temperature of earth surface and air (Sherwood et al., 2010). The results show high values of RH%
276 70.1% (85%) in winter (summer) season for PCs over Gandhi College. Conversely, notable
277 fluctuations in RH% are observed over the coastal city, Karachi, with values of 71.5% (65.9%) in
278 winter (summer). Similarly, Fig. 2S and Table 2S show the LTS conditions for PCs and NPCs. The
279 high LTS values indicate more stable condition over Dhaka. Similarly, Table 2S shows the seasonal
280 average values for other meteorological parameters. The results indicate high values of T_{850}, RH%
281 and Ω **295.5 (297.5)** K, 88.8 (83.5)% and -0.19 (-0.17) m/s respectively for PCs (NPCs) for over
282 Patna in summer.

283 Besides, during the last two decades, the wv and fog over the Arabian Sea were increased (Verma
284 et al., 2022). Therefore, the high values of wv and RH% in summer months is due to the high-
285 speed zonal winds that blew in the summer season and transport water vapors and sea salt from
286 the surface of the Arabian Sea and hydrophilic aerosols such as soil dust from deserts of Iran,
287 Pakistan, and India to IGP. Moreover, during the winter season, the elevated humidity levels are

288   noticeable over IGP, particularly in the vicinity of Gandhi College. This increased humidity is a

289   result of evapotranspiration driven by agricultural practices, irrigation, the presence of rivers and

290   lakes, and the introduction of moist, cold air from western winds (Nair et al., 2020). Where $\Omega < 0$

291   for PCs over all study areas except Karachi.

292   The distinct variations in meteorological parameters reveal the occurrence of clouds with diverse

293   properties. The detailed analysis of such clouds is given in the next subsections.

294
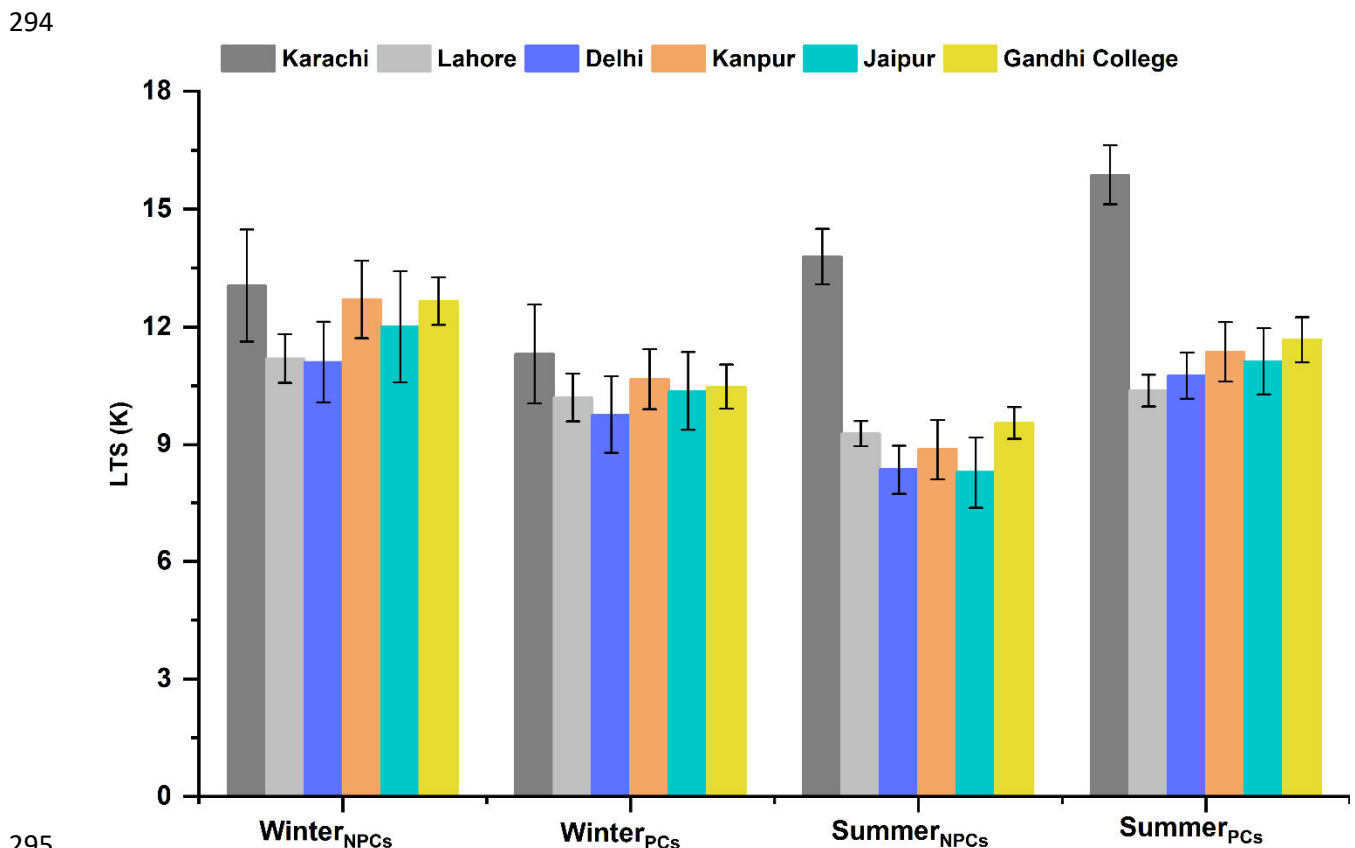
295

296   **Figure 4.** Variations in lower tropospheric stability (LTS) over all study sites for PCs and NPCs in winter and summer
297   seasons, the error bars show the standard deviation (SD) values.

298 **Table 2.** Meteorological parameters for PCs(NPCs) in summer and winter seasons. Maximum values are for both types of clouds shown in bold
299 and minimum values are indicated as italic.

	Winter Season			Summer Season		
	T_{850} (K)	RH%	Ω (m/s)	T_{850} (K)	RH%	Ω (m/s)
Karachi	**284.6 (285.8)**	**71.5** (38)	-0.038 (*0.030*)	*295.9* (298.8)	65.9 (45.9)	*0.005* (-0.003)
Lahore	*280.5 (281.2)*	*59.5* (35.5)	*-0.02* (**0.065**)	**298.3 (300.2)**	65 (*33.5*)	-0.028 (*0.025*)
Delhi	284.2 (283.1)	60.2 (*33.8*)	**-0.1** (0.04)	296.5 (299.4)	64.2 (42)	-0.05 (*-0.001*)
Kanpur	283.8 (284.1)	65.7 (36)	**-0.1** (0.048)	296.5 (298.4)	73.7 (43.6)	-0.13 (-0.08)
Jaipur	283.9 (284.1)	66 (40.5)	-0.065 (0.049)	296.8 (298.7)	*64* (**51.7**)	-0.04 (*-0.029*)
Gandhi College	283.2 (284.1)	70.1 (**45.7**)	**-0.1** (0.05)	296.9 (*298.3*)	**85** (42.5)	***-0.16 (-0.11)***

300

301

302

303

304

3.3. Regional and seasonal distribution of clouds and precipitations

3.3.1. Regional and seasonal differences in clouds occurrence and its microphysical structure

Fig.5 shows the frequency of occurrence of precipitable clouds and total number of cloudy days. Chen et al. (2018) suggested the COT to be the effective measure for assessing the clouds and potential for precipitation. In our case, to avoid any overestimation, the COT data are aligned with PR data on corresponding dates and then filtered to include COT ~ > 5 for PCs. The results show that in the winter season the frequency of clouds is low over Karachi and high over Lahore and Gandhi College. The results suggest the high number of PCs only over Lahore. In summer season, the high number i.e., 74 % of the total data counts over Gandhi College are identified as cloudy days, 60 % of which are PCs. Similarly, most of the clouds over Lahore, Delhi and Jaipur are PCs. Conversely, the least number of PCs (6 %) are found over Karachi. Likewise, Fig. 3S shows the total number of cloudy days and the number of days on which PCs occurred. The high occurrence of clouds is observed over Kolkata 83% (60%) and Dhaka 91% (69%) in summer (winter) season. The high occurrence of PCs in summer is due likely to the significant impact of elevated aerosols with the southwesterly winds on the summer monsoons and occurrence of PCs. Therefore, Kolkata and Dhaka are of critical importance from perspective of aerosol loading and ACI (Dahal et al., 2022).
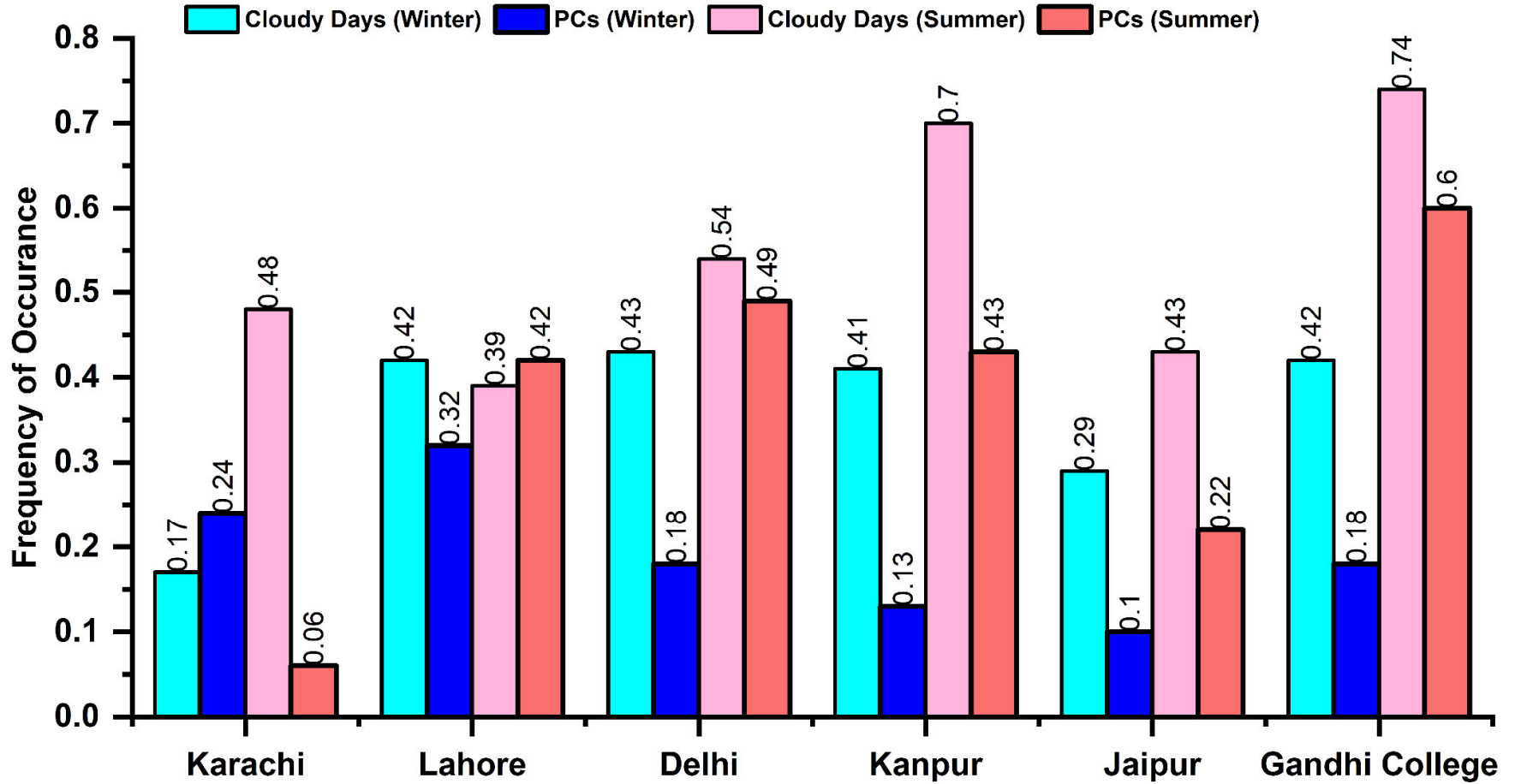
Figure 5. Frequency of occurrence of total cloudy days (including PCs and NPCs) and only PCs is shown for both winter and summer seasons.

327 Table 3 shows the criteria adopted from previous papers (Rossow & Schiffer, 1999; Wyant et

328 al., 2006; Sharma et al., 2023) for further classification of NPCs and PCs into different type of

329 clouds. The aim of identifying the cloud types is to assess the cloud regimes and their vertical

330 structure for the better understanding of ACPI. In accordance with table 3, Fig. 6 shows joint

331 histograms of COT-CTP displaying the median values of CF for nine different types of clouds.

332 For a quick visual comparison, the cloud types are ordered from low to high level clouds. Also,

333 for each histogram, the bins of COT and CTP are located on x- and y-axis respectively. While

334 the CF of each bin is represented with the colored bar with its value mentioned in the

335 histograms as shown in Fig. 6.

336 The results exhibit noticeable differences in the pattern of cloud regimes over all study areas.

337 The diverse CF values are observed in winter and summer seasons for NPCs and PCs over

338 Karachi. In winter season, only stratus NPCs ($23 < COT < 60$, $800 > CTP > 680$ hPa) are

339 dominant with CF ~ 0.9. While, in summers, high value of CF ~ 0.9 for low and intermediate

340 thickness of high-level clouds such as Cirr-Stratus NPCs ($3.6 < COT < 23$, $180 < CTP < 440$

341 hPa) are observed. Similarly, the type of PCs in both summer and winter season that occurred

342 with CF ~1.0 include cirrus and cirr-stratus. The relatively reduced value of CF for thick NPCs

343 in winters and PCs in summers is attributed to the low values of AOD and high values of LTS.

344 The results depicted slight differences and similarities in CF values for thick and thin NPCs

345 respectively in winter season for all areas except Karachi. Besides, the high-level PCs are

346 identified in the two bins of CTP ($180 < CTP < 440$ hPa) and ($440 < CTP < 680$ hPa) over all

347 study areas. The formation of these similar types of PCs in winters are associated with the

348 similarities in Ω, LTS values and aerosols concentration.

349 Likewise, in summer season, the matrices of PCs and NPCs exhibit a wide range of cloud types.

350 However, the CF values are comparatively high for PCs. Most of the identified PCs are formed

351 in the two bins of CTP ($180 < CTP < 440$ hPa) and ($440 < CTP < 680$ hPa) with CF values

352 ranging from 0.8 to 1.0. The results suggest low values of CF for the low-lying thick NPCs

353 over all study areas. Moreover, the results illustrate a more frequent occurrence of all the three

354 types of thick NPCs in one bin of COT ($23 < COT < 60$) and all the three types of high-level

355 NPCs for CTP ($180 < CTP < 440$ hPa) over Delhi, Kanpur, and Gandhi College. Therefore,

356 these are considered the cloudiest regimes. Besides, contrasting regional variations are also

357 observed in PCs. The maximum CF values for all types of PCs are observed over Kanpur and

358 Gandhi College. Similarly, relatively good values of CF in a bin of COT ($23 < COT < 60$) and

359 a bin of CTP (180 < CTP < 440 hPa) over Lahore, Delhi, and Jaipur depict the frequent

360 occurrence of thick and high-level PCs respectively. In addition, among all the estimated low-

361 level PCs, cumulus and strato-cumulus exhibit good CF values (0.7) over Kanpur and Gandhi

362 College. The formation of thick clouds can be attributed to the enhanced convection process

363 due to the atmospheric instability.

364

365 **Table 3.** Classification of clouds based on CTP – COT joint histograms.

CTP (hPa)	COT		
	0-3.6	3.6-23	23 to >60
440 to <180	Cirrus	Cirr-Stratus	Deep convection
680-440	Alto-Cumulus	Alto-Stratus	Nimbo-Stratus
<800 to 680	Cumulus	Strato-Cumulus	Stratus

366

367
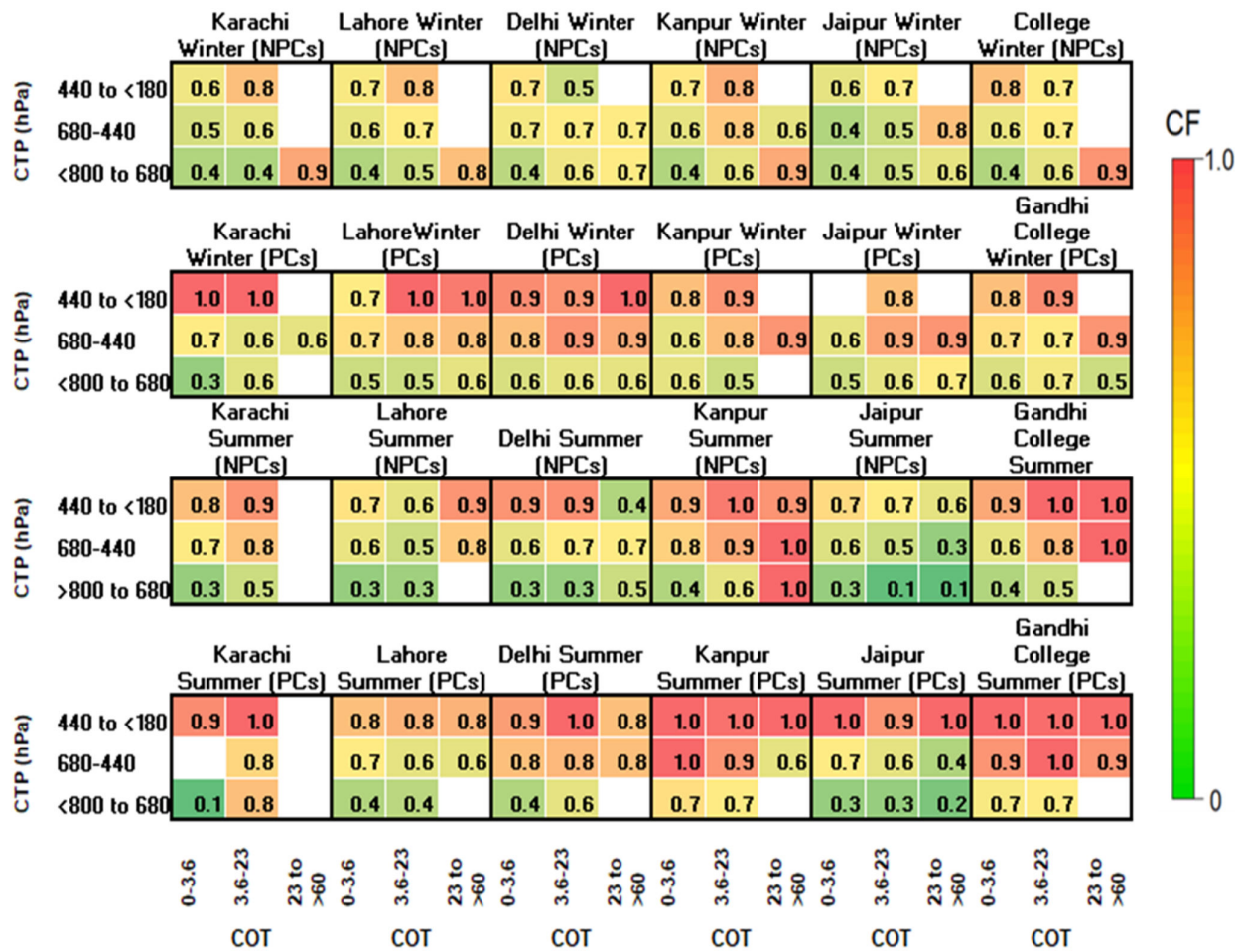
Figure 6. Types of NPCs and PCs in winter and summer season

369   After estimating the cloud types, Fig. 7 shows the probability distribution function (PDF) of

370   cloud microphysical properties for the identification of differences in microstructure of NPCs

371   and PCs in summer and winter seasons. From the results it is depicted an approximately similar

372   pattern for the CER of NPCs in winter. However. the clouds have high peaks of PDF for lower

373   values of CDNC over Karachi. The low number of CDNC results in thin NPCs as shown in

374   Fig.7. Similarly, Fig. 7(c and g) shows the microstructure of NPCs in summer. The results

375   indicate that as compared to CER values in winter, the probability of CER >~15 µm is high in

376   summer season. However, high peak for CER < 15 µm is observed over Karachi. Similarly, the

377   CDNC shows a high probability for CDNC > 50 cm^{-3} with the high PDF values over Karachi.

378   Where, the lowest number of CDNC is observed over Lahore indicating the formation of high-

379   level thin NPCs in summer.

380   Fig. 7(b and f) shows the distribution pattern of CER and CDNC of PCs in winter season. It is

381   clearly observed that the distribution of CER for PCs is like those for NPCs in winter season.

382   However, PDF have peak values for relatively higher CDNC, which illustrates the occurrence

383   of thick clouds. Fig. 7(d and h) shows the variations in CER and CDNC in summer season. The

384   results show a wider distribution for CER > ~15 µm and higher peaks for CDNC > ~ 50 cm^{-3}

385   suggesting the formation of thick PCs in summer as shown in Fig.6.

386

387
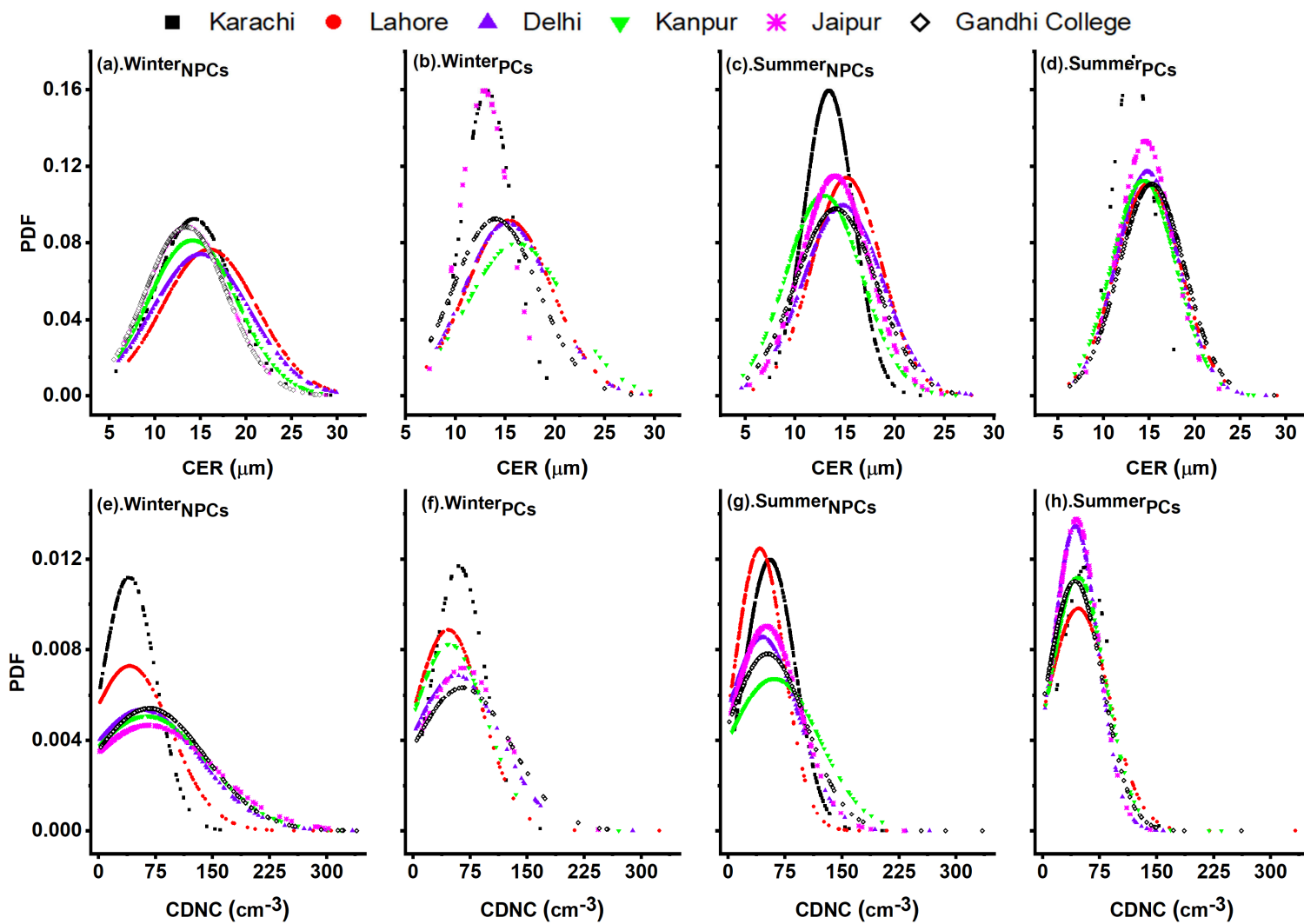
388

389 **Figure 7.** Probability density function (PDF) of precipitating (PCs) and non-precipitating clouds (NPCs) in winter and summer season

3.4. Aerosol-Cloud-Precipitation Interaction (ACPI)

In the following sections, ACPI is analyzed and discussed in detail for PCs and NPCs in summer and winter seasons.

3.4.1.   Aerosol effects on cloud properties

The impact of aerosols on CDNC and CER of PCs and NPCs is illustrated as scatter plots in Fig. 8-9. The quantification of the AOD-CER and AOD-CDNC relationships is demonstrated through detailed linear regressed slopes, regression coefficients (R^2) and Pearson's correlation coefficient (R). The color bar represents the variations in LTS. The results show that the two-sample student's t test is carried out to analyze the AOD-CER and AOD-CDNC relationship in view of statistics. The results illustrate that the relationships are statistically significant at 95% ($p < 0.05$) significance level for all study areas. Fig.8 shows that in winter season, the AOD-CER correlation is good for PCs and weak for NPCs. The results also show that the LTS values are higher for NPCs. The weak AOD-CER correlation may be linked to the inhibition of droplet growth due to less soluble aerosols, originated from biomass burning (Kang et al., 2015). In our case, all the selected study areas are among the most urbanized and industrialized areas of IGP. Therefore, most of the prevailing aerosols are the less soluble soot and BC particles. That weakened activation of cloud droplets, inhibits the formation of PCs and evaporate to higher altitudes and thereby increases the droplet residence time (Kumar & Physics, 2013). Besides, the results show a contrasting pattern of LTS values. Although, RH over Karachi (38.3±9 %) is higher than over the other study areas (shown in Table 2), the negative AOD-CER correlation is observed over Karachi due to its coastal location, the low value of AOD and high level of LTS.

Fig. 9 illustrates the AOD-CER and AOD-CDNC correlation in summer season. The results depict a more significant and positive AOD-CER correlation in summer season than winter season. Unlike winter season, the high LTS values are observed for PCs. Yuan(2008) associated the positive AOD-CER correlation to the soluble organic aerosols. Myhre et al. (2007) hypothesized that the positive AOD-CER correlation is a maximum for low CTP and minimum for high CTP. Hence, in our study, referable to the approximated CF values shown in Fig.6, the significant and positive AOD-CER correlation under unstable atmospheric conditions resulted in thick and high-level clouds. Furthermore, it is observed that CER and CDNC values for NPCs increase with increasing instability. Meanwhile, the enhanced process of droplet activation may result in large AOD, higher CER, giant and fewer CCN (Yuan, 2008).

422 Therefore, the weak correlation of AOD with CER and CDNC may be due to the
423 anthropogenically ejected water-soluble organic aerosols and a smaller number of CCN.

424 Fig. 5S and 6S show the impact of AOD on CER and CDNC for PCs and NPCs in winter and
425 summer respectively. The results indicate a positive and weak AOD-CER correlation 0.2, 0.07
426 and 0.004 for NPCs over Kolkata, Dhaka and Patna respectively and for PCs (0.08) over both
427 Kolkata and Patna. Similarly, a positive and weak AOD-CDNC is observed over all areas for
428 PCs. Likewise, Fig. 6S also illustrates weak AOD-CER correlation is 0.06, 0.2 and 0.12 for
429 both types of clouds in summer. As compared to other areas, the correlation analysis is less
430 significant over Karachi, Kolkata, Dhaka and Patna. This can be attributed to the persistence
431 of diverse aerosol types influenced by their coastal locations, different meteorology and the
432 alternating inflow and outflow of easterly and westerly winds.

433 Recent advances in remote sensing led to cost-effective solutions and an increase in available
434 data at various temporal and spatial resolution to bridge scientific gaps among different
435 disciplines. While satellite-based retrievals have many advantages over in-situ and ground-
436 based measurement such as broader regional coverage and enhanced spatial resolution, they
437 are still prone to considerable uncertainties owing to the indirect nature of remote-sensing,
438 retrieval algorithms, thermal radiance, infrequency of satellite overpasses, and cloud top
439 reflectance (Hong et al., 2006;Tian et al., 2010; Hossain et al., 2006). In our study, apart from
440 the aforementioned factors contributing to the uncertainty, any residual cloud contamination
441 could also lead to biased retrieval of AOD. Likewise, satellite-based retrievals for cloud
442 properties are crucial to understanding the pivotal role of clouds in climate and the role of
443 clouds is still a dominant source of uncertainty in prediction of climate change. These,
444 uncertainties in AOD and retrievals of cloud properties also propagate through the modeling
445 process, potentially leading to less accurate climate predictions. Likewise, these uncertainties
446 appeared to influence the findings in the current investigation. For instance, a limited
447 correlation between AOD and CER is observed over Lahore, particularly in cloudier regimes
448 as depicted in Fig. (5-6). This contrasts with robust impacted documented in the earlier studies
449 (Michibata et al., 2014). However, high sensitivity of SIE is observed for PCs particularly in
450 winter season indicating the delay in onset of precipitation and more retention of clouds.
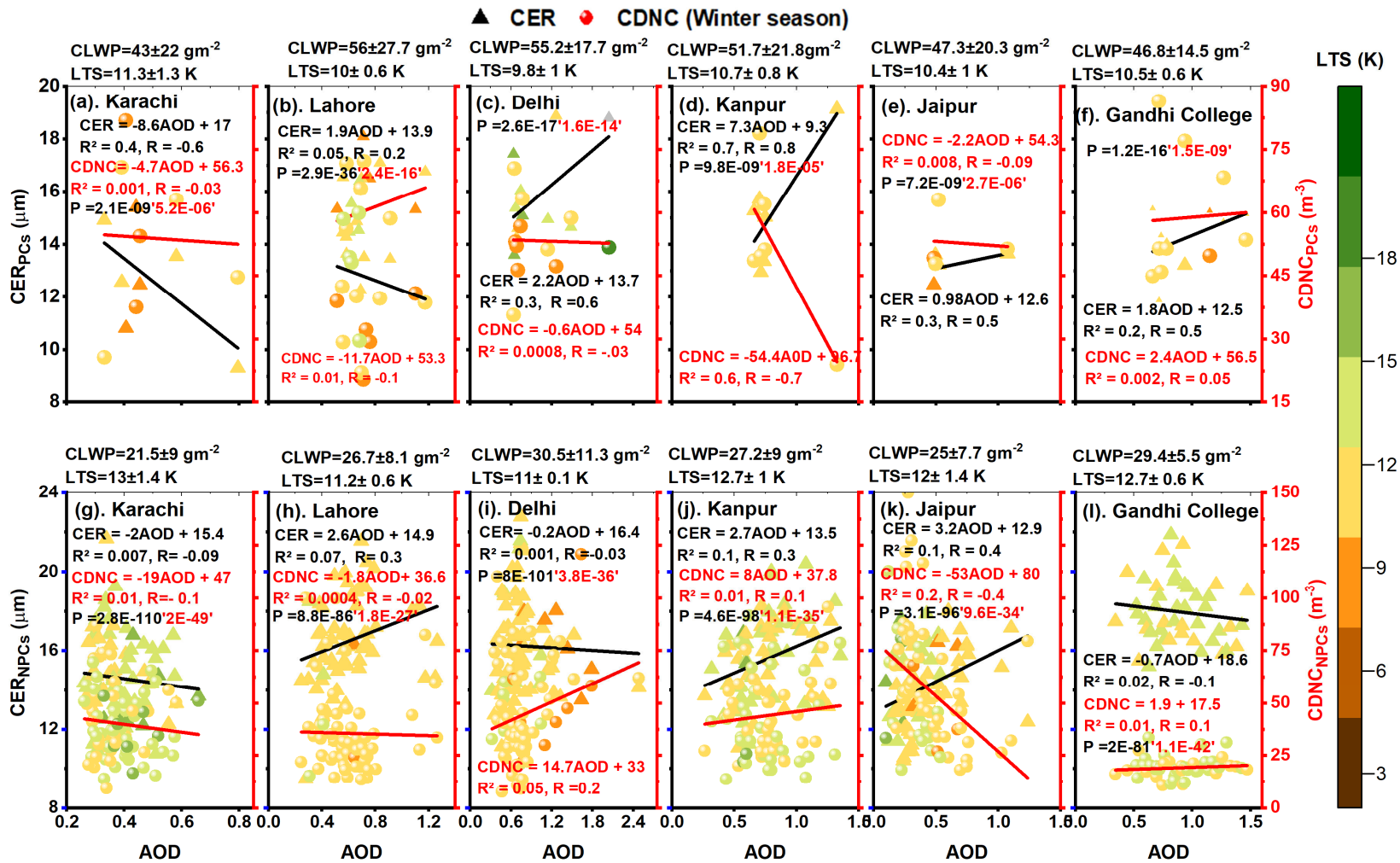
Figure 8. AOD-CER and AOD-CDNC regression and correlation coefficient considered at 95% confidence level for PCs and NPCs over all study areas in winter season.
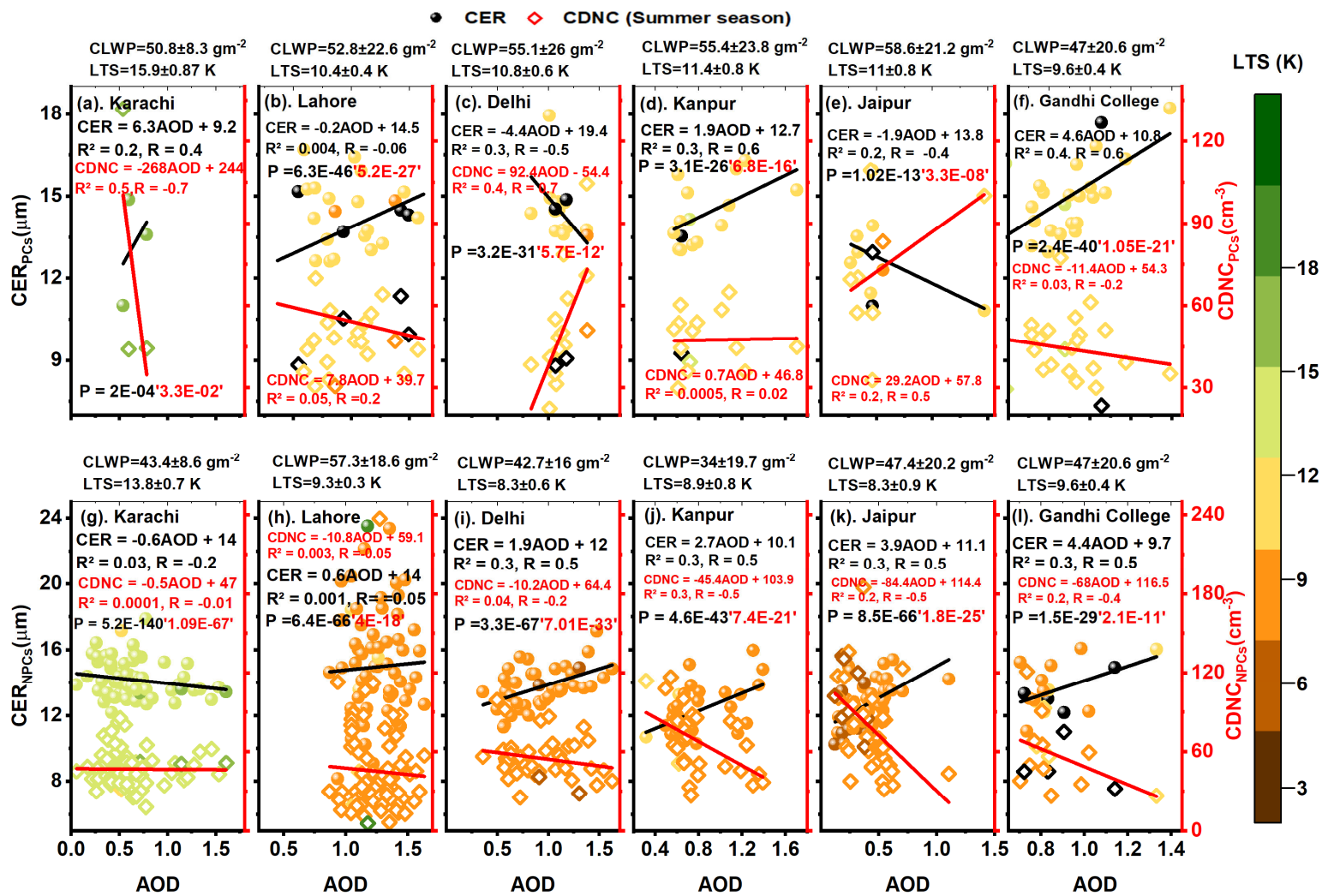
Figure 9. Same as Fig. 8 but in summer season.

456 *3.4.2. Seasonal variations in sensitivities of aerosol-cloud indirect effects and ACI*

457 Fig.10 shows assessment of four ACI sensitivities in terms of CDNC using daily mean values

458 of MODIS observations available over the entire study area. Since, studying the effects of

459 aerosols on the co-located clouds is a challenging task due to the overestimation of thin clouds

460 in AOD retrievals. Therefore, to minimize the propagation of AOD retrieval errors in ACI, the

461 current study attempted to estimate the sensitivities of different cloud mechanisms to CDNC.

462 The sensitivity of CER to CDNC is assessed as a signature of FIE as shown in Fig.10a. The

463 positive values illustrate that CER decreases with an increase in CDNC revealing the

464 occurrence of the Twomey effect. Whilst the negative values depict the anti-Twomey effect.

465 Tripathi et al., (2007) divided IGP into four regions as western, central, eastern part of IGP and

466 the foothills of Himalayas. Their results depicted high concentration of dust in western part,

467 and an increase in anthropogenic aerosols as one moves from western to eastern part of IGP.

468 Therefore, they attributed the resulted strong indirect effect in winter to the high concentration

469 of regional anthropogenic pollution. However, in our case, the FIE is investigated for both PCs

470 and NPCs in both seasons. The resulted approximations in winter season show strong (weak)

471 sensitivity of FIE for PCs (NPCs). Similarly, the estimated sensitivity of FIE for all NPCs and

472 PCs is also positive in the summer season. Fig. 7S(a) shows sensitivities for FIE in both seasons

473 for PCs and NPCs. The results indicate high values of sensitivity FIE in winter season which

474 is similar to the results for Karachi, Lahore, Delhi and Kanpur as shown in Fig. 10 a. This is

475 attributed to high level of aerosol emission from residential heating and industrial activities.

476 Furthermore, the results illustrate higher values of FIE in summer. This is attributed to the

477 massive aerosol loading due to aerosol carried by winds and originated by anthropogenic

478 activities and unstable meteorology.

479 Fig. 10b illustrates the sensitivity of CLWP to CDNC as a proxy for evaluation of the SIE or

480 lifetime effect. The positive sensitivity estimated for all NPCs and PCs suggested that the

481 CLWP increase with increase in aerosol. Further, the results show that the sensitivity of SIE is

482 stronger for PCs in winter which indicate the delay in onset of high PR. Similarly, the results

483 show that the SIE sensitivity values are higher for PCs than for NPCs in the corresponding

484 seasons. Therefore, the results depict that the lifetime of PCs is greater than NPCs. Which is

485 attributed to the high level of RH for PCs as shown in Table 2. Fig. 10 (a and b) shows that the

486 FIE sensitivities are weaker than SIE.

487   Fig. 10c shows the TIE in terms of the sensitivity of COT to CDNC. The results illustrate
488   positive values of sensitivity for all NPCs and PCs which indicate that COT increases with
489   increase in aerosol concentration. The results also reveal that sensitivity of TIE is a linear sum
490   of the sensitivities of FIE and SIE. Further, the results also suggest that the variations in TIE
491   sensitivity are largely dependent on SIE.

492   Fig.10d shows the sensitivity of CDNC to AOD as an estimation of ACI in terms of CDNC.
493   The positive values show the increase in CDNC with the increase in AOD. Therefore, positive
494   ACI reflects the inhibition of precipitation formation. Whilst, the negative values illustrate the
495   decrease in CDNC and enhanced PR (Fan et al., 2018). The results depicted relatively large
496   and positive sensitivities for NPCs in winter over Lahore, Delhi, and Kanpur, which inhibits
497   the onset of rainfall. The Sensitivity of ACI for NPCs in summer is positive over Karachi and
498   Lahore and negative over Delhi, Kanpur, Jaipur, and Gandhi College. Ackerman et al. (2004)
499   associated the negative ACI_{CDNC} to the wet scavenging and mixing of air by entertainment. In
500   our case, negative ACI may be due to the growth of CER and decrease in CDNC with aerosol
501   loading under unstable conditions(shown in Fig. 9). Further, the magnitude of sensitivity for
502   PCs in summer is low. Which can be due to the droplet growth through collision coalescence
503   and wet scavenging in thick clouds, decreased dependency on CCN.

504

505
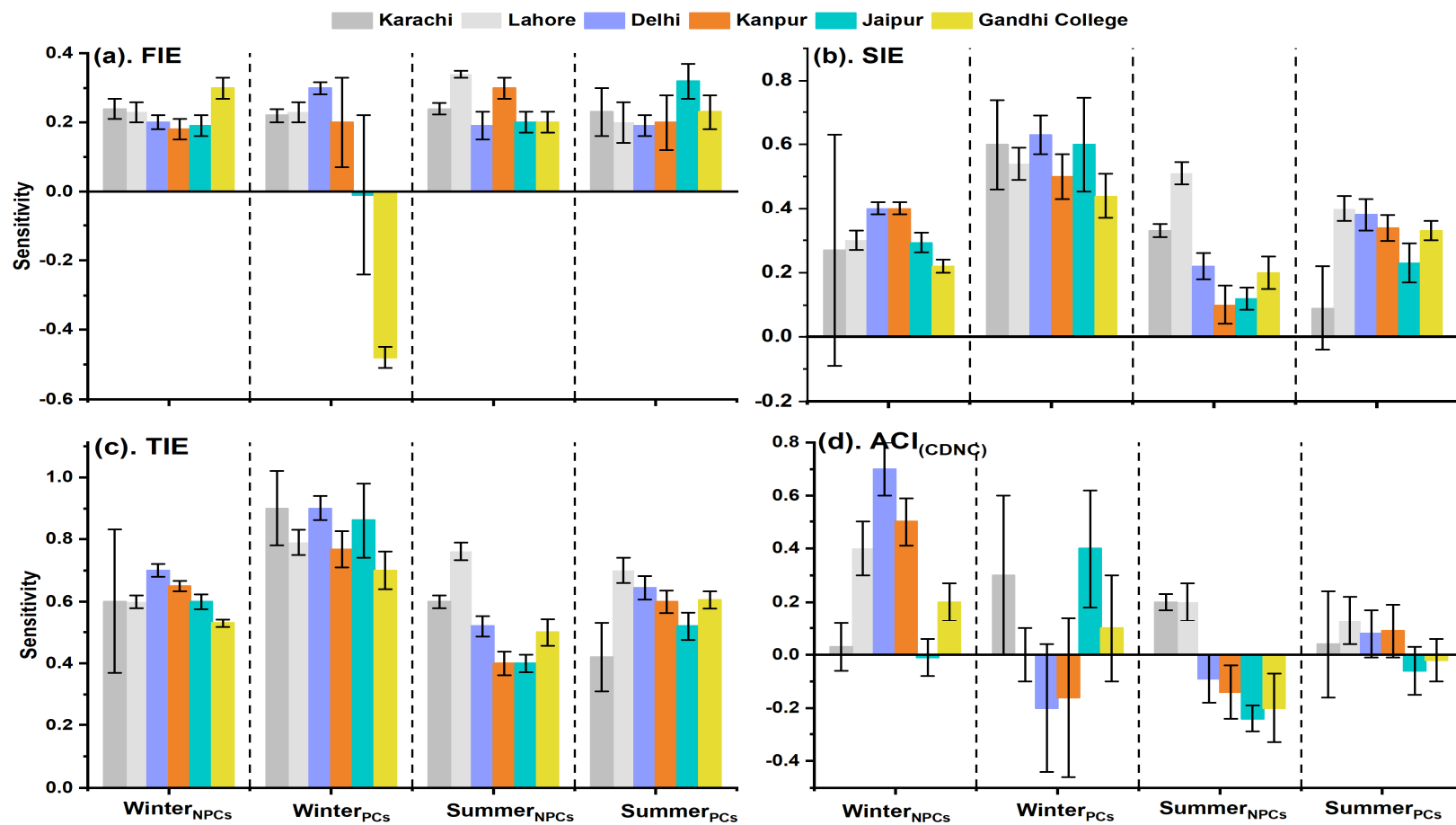
Fig. 10. The sensitivity metrices estimated for aerosol-cloud relationship using CDNC is shown in (a) FIE $= -\left(\frac{\partial ln\,(CER)}{\partial ln\,(CDNC)}\right)$ (b) SIE $= \left(\frac{\partial ln\,(cLWP)}{\partial ln\,(CDNC)}\right)$, (c) TIE $= \left(\frac{\partial ln\,(COT)}{\partial ln\,(CDNC)}\right)$ and (d) ACI $= \left(\frac{\partial ln\,(CDNC)}{\partial ln\,(AOD)}\right)$. Where, the error bars show the standard deviation (SD).

509   *3.4.3. Aerosol effects on precipitation*

510   Fig. 11 shows the average values of PR in mm/day retrieved from TRMM. The results show

511   an obvious seasonal difference in precipitation occurrence. The reason for the high (low) PR

512   values is due to the suitable meteorological condition including high (low) LTS values for PCs

513   in summer (winter) season (shown in Fig. 8-9). The stable atmospheric condition with high

514   LTS value in winter serves to inhibit the convection process and have a significant impact on

515   controlling the PR in winter (Zhao et al., 2006). Conversely, during summer season, the

516   meteorological instability prevails with low LTS values which result in high RH. This not only

517   causes enhanced AOD due to the water uptake and resulted swelled hydrophilic aerosols (Alam

518   et al., 2010; Alam et al., 2011) but also affects the cloud and precipitation formation due to the

519   enhanced evaporation and convection. Additionally, Fig. 8-9 also show evidently and

520   specifically during summer that the possible cause of positive AOD-CER correlation is the

521   negative AOD-CDNC correlation under unstable meteorology over all areas except Karachi.

522   As a result, Fig. 11 shows high (low) values of PR over all areas with maximum over Gandhi

523   College (Karachi). The results show high (low) approximation of PR over Gandhi College

524   (Karachi). Knowing that the rate of conversion of CDNC to precipitation is proportional to

525   CER (Wolf & Toon, 2014). Therefore, the high PR values is due to the growth of bigger cloud

526   droplets in summers. Further, apart from the reasons mentioned in the preceding sections, the

527   other justification for the differently perturbed aerosols, clouds and precipitation pattern over

528   the study areas in summers is due to the entrance of southeast winds from Bay of Bengal

529   passing across Gandhi College to Delhi and Lahore and entrance of same winds from Arabian

530   sea to Pakistan through Karachi (Anwar et al., 2022).

531   Fig. 12 shows scatter plots of PR verses CDNC. The plot is colored with COT to examine the

532   impact of CDNC on PR for similar macrophysics. When CDNC are few, then the COT are

533   sparse that grow larger, form less reflective clouds and precipitate faster (Kump & Pollard,

534   2008). The same phenomenon seems true in our case. The results illustrate high PR (0.0007

535   mm/day) values for clouds with COT ranging from 3 to 28 with CDNC $< \sim 50$ cm^{-3} and

536   intermediate for optically thick clouds and CDNC $> \sim 50$ cm^{-3} in both seasons.

537
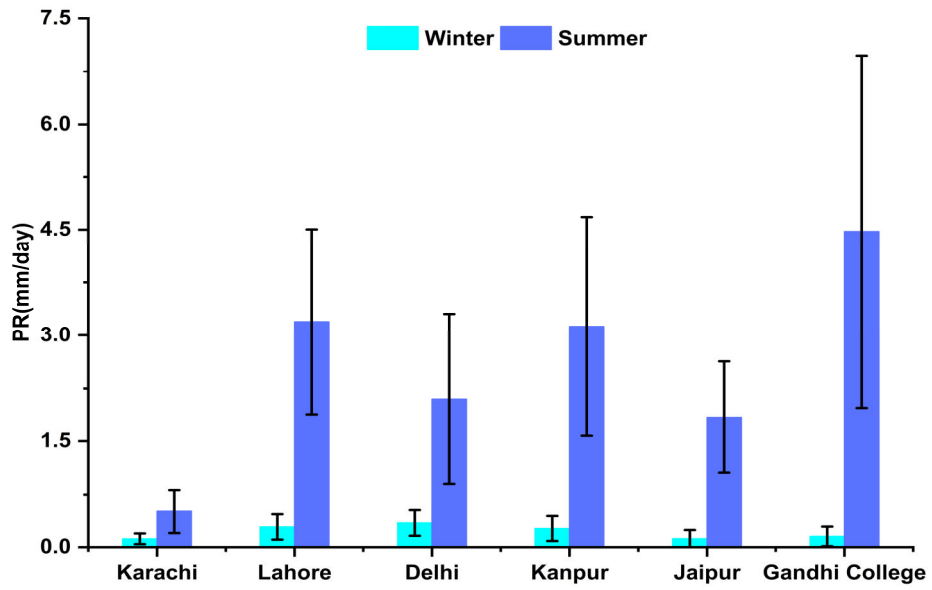
Figure 11. Mean Precipitation rate (PR) for the PCs in winter and summer season and SD values with 95% confidence interval.
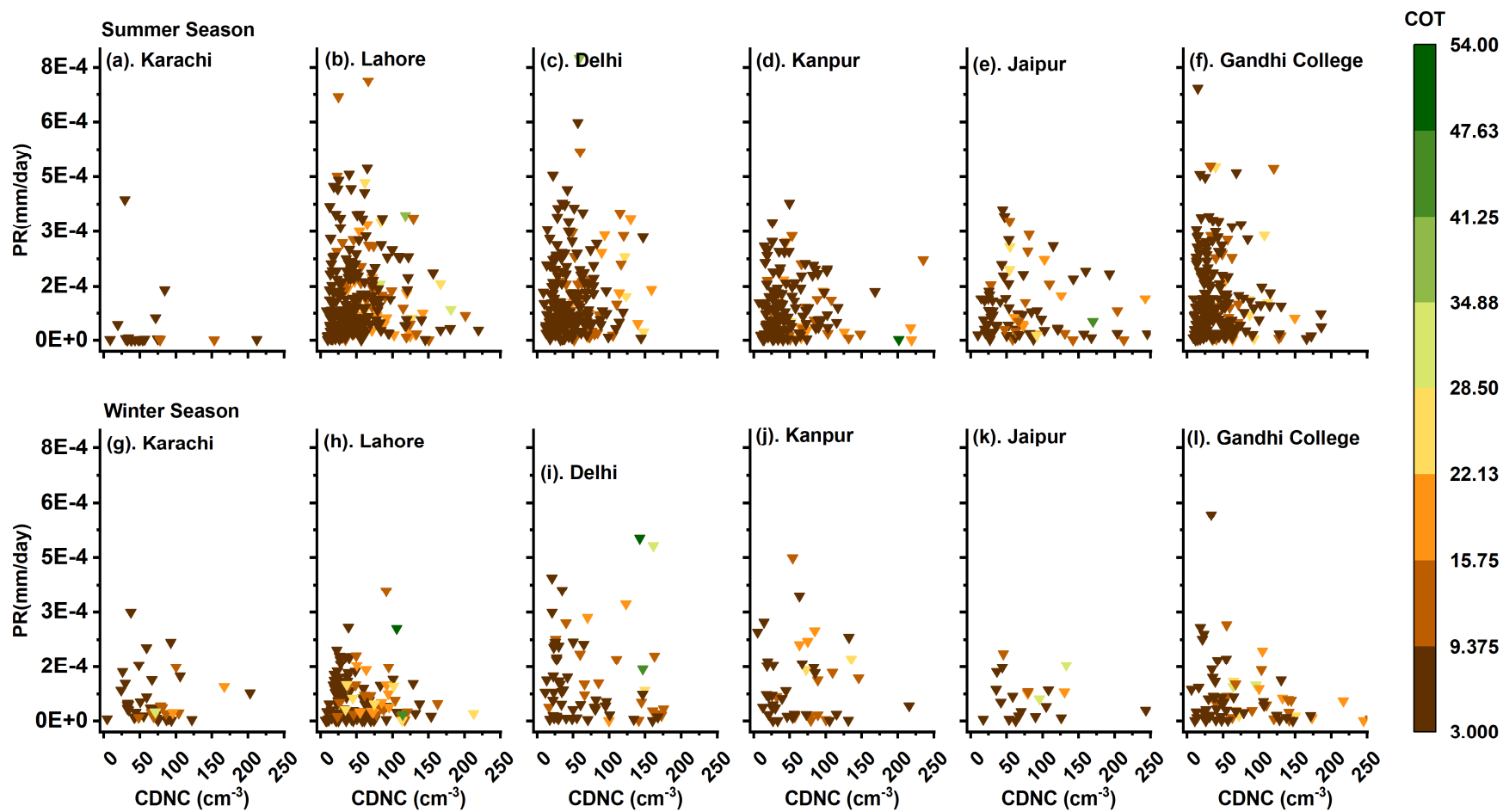
Figure 12. Scatter diagrams of PR (mm/day) verses CDNC (cm^{-3}) in summer and winter seasons. color coding shows the COT of PCs.

540

541

542

543   Fig.13 shows the sensitivity (S_o) of PR to CDNC defined by $S_o = \left(-\dfrac{dln(PR)}{dln\,(CDNC)}\right)_{COT}$ for clouds

544   of low and intermediate thickness illustrated in Fig. 13 a and Fig. 13 b respectively. However,

545   sensitivity analysis for COT > 23 could not be performed due to less number (0 to 04) of

546   available samples. In the sensitivity equation the minus sign shows the suppression of

547   precipitation formation due to the increase in CDNC. Further, when S_o is positive, correlation

548   between PR and CDNC is negative; however, for negative S_o, PR and CDNC are positively

549   correlated. The results show peak values of S_o i.e., 0.7 ± 0.3, 0.6 ± 0.3, 0.5 ± 0.3, and 0.4 ±

550   0.4 over Jaipur, Delhi, Gandhi College and Karachi respectively at intermediate values of COT

551   in winter, indicating the occurrence of lightly precipitating clouds. Referable to Fig. 13b, the

552   low magnitude of S_o 0.2 ± 0.3 and 0.08 ± 0.2 over Kanpur and Lahore respectively is due to

553   coagulation, in which precipitations are less sensitive to CDNC.

554
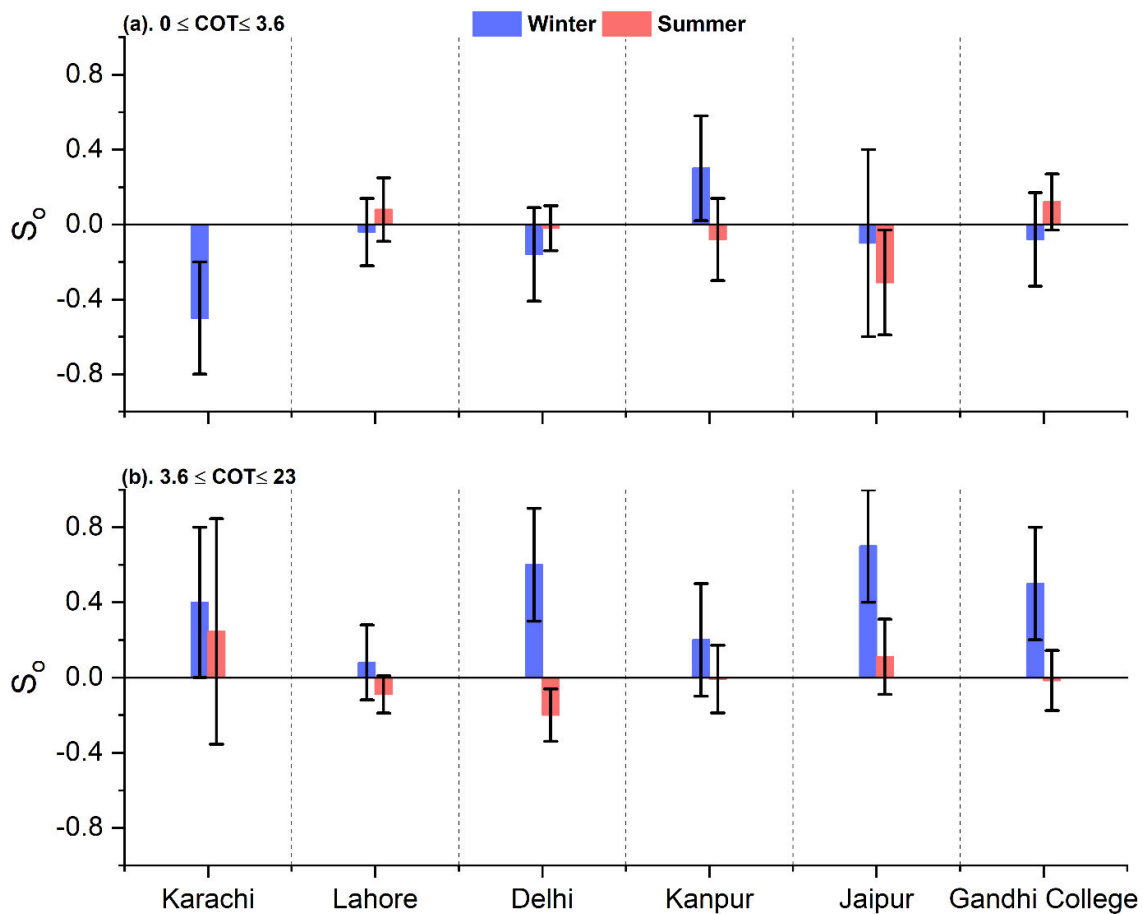
555

556   **Figure 133.** Sensitivity 'So' of precipitation rate (PR) for two bins of COT shown in (a). 0 ≤

557   COT ≤ 3.6 and (b). 3.6 ≤ COT ≤ 23.

558

4. Conclusion

In this study, the long-term (2001-2021) data retrievals from MODIS coupled with TRMM and NCEP/NCAR reanalysis-II datasets over the entire study area are compiled and analyzed for PCs and NPCs in winter and summer season. The following are the main findings of this study.

A decadal decrease in AOD is observed over Karachi (-1.9%) and Jaipur (-0.5%). Meanwhile, AOD exhibits an increase over Lahore (5.2%), Delhi (9%), Kanpur (10.7%) and Gandhi College (22.7%). The LTS values are High (low) for NPCs (PCs) in winter and for PCs (NPCs) in summer season. However, among all study areas, Karachi exhibits comparatively high LTS values in both seasons. Apart, the increase in RH% for PCs ranged from 33-57% in winter and from 25-45 % in summer. $\Omega > 0$ for all NPCs in winter and < 0 for PCs in both winter and summer seasons.

In winter season low frequency of cloudy days over Karachi and high over Lahore and Gandhi College is estimated. Also, the high number of PCs are estimated only over Lahore. In summer season, out of the 74 % of the cloudy days , 60 % are PCs over Gandhi College. Similarly, most of the clouds over Lahore, Delhi and Jaipur are PCs. Conversely, the least number of PCs (6 %) is found over Karachi. The high-level PCs are identified in one bin of CTP ($180 < $ CTP $ < 440$ hPa) over all study areas in winters. In summer season, all the three types of high level and thick PCs have significant values of CF. The low-level PCs are identified as stratus clouds. Further, PDF values for CER $> \sim 15$ μm and CDNC $> \sim 50$ cm^{-3} for NPCs and PCs is high (low) in summer (winter) over all areas except Karachi.

The AOD-CER correlation is good for PCs and weak for NPCs in winter season. Also, the CER and CDNC values increase with increase in LTS. The sensitivity value of FIE is high (low) for PCs (NPCs) in winter. Further, magnitude of sensitivity of FIE (SIE) is low (high). Also, the sensitivity of TIE is a linear sum of the sensitivities of FIE and SIE. Further, ACI sensitivity values for PCs in summer are small, illustrating less dependency of CER on CDNC in thick clouds.

The high (low) PR values are observed in summer (winter). Further, high PR values for comparatively thin clouds with fewer CDNC $< \sim 50$ cm^{-3} and intermediate for optically thick clouds and CDNC $> \sim 50$ cm^{-3} are observed. Sensitivity values are small (high) for thick clouds in summer (winter).

Being one of the major source regions of anthropogenic aerosols across the globe, IGP offers interesting insights into the study of ACPI coupled with aerosol indirect effects. This study highlights that the aerosol-cloud relationship exhibits different behavior under different meteorological conditions, at coastal and inland locations. Thus, compared to other study areas, the stable atmospheric conditions due to the constant sea breeze weakened the ACI over Karachi, which resulted in a smaller number of CDNC, NPCs, and PCs. Further, our study also provides a very good platform for the detailed analysis of sensitivity tests of aerosol indirect effects and precipitation formation.

Limitations and future recommendations:

Although the current study is as thorough as possible, however, it has its limitations due to the topographical complexity of IGP, the lack of in-situ measuring instruments in Pakistan, and the intrinsic uncertainties associated with satellite-based data. Therefore, simulations of ground-based measurements along with satellite-based retrievals and calculation of cloud properties and CCN by different Community Atmosphere Model (CAM) and Weather Research and Forecasting (WRF) Models are recommended for deep insight into the various mechanisms of ACPI over IGP.

Data Availability: The MODIS and TRMM data can be obtained from the NASA Goddard Earth Sciences Data and Information Center (GES DISC) and can be retrieved from the websites: https://modis.gsfc.nasa.gov/data/ and https://gpm.nasa.gov/data . The reanalysis-II datasets are obtained from the website: https://psl.noaa.gov/data/gridded/data.ncep.reanalysis2.html . The processed data used in this work are available on reasonable request from the corresponding author.

Author contribution: NG processed and analyzed the data and wrote the original draft of the manuscript. KA proposed the Idea, supervised this work and revised the manuscript. YL helped in revising the manuscript.

Acknowledgment: The authors gratefully acknowledge the NASA Goddard Earth Sciences Data and Information Services Center (GES DISC) for the provision of freely available data retrieved from MODIS and TRMM. We are also grateful to the NOAA Physical Sciences Laboratory (PSL) for free accessibility to (NCEP/NCAR) reanalysis-II datasets.

References

Ackerman, A. S., Kirkpatrick, M. P., Stevens, D. E., & Toon, O. B.: The impact of humidity above stratiform clouds on indirect aerosol climate forcing, *Nature., 432*, 1014-1017, https://doi.org/10.1038/nature03174 , 2004.

Alam, K., Iqbal, M. J., Blaschke, T., Qureshi, S., & Khan, G.: Monitoring spatio-temporal variations in aerosols and aerosol–cloud interactions over Pakistan using MODIS data, Adva. Space Res., *46*, 1162-1176, https://doi.org/10.1016/j.asr.2010.06.025, 2010.

Alam, K., Qureshi, S., & Blaschke, T.: Monitoring spatio-temporal aerosol patterns over Pakistan based on MODIS, TOMS and MISR satellite data and a HYSPLIT model, Atmos. Envi., *45*, 4641-4651, https://doi.org/10.1016/j.atmosenv.2011.05.055, 2011.

Albrecht, B. A.: Aerosols, cloud microphysics, and fractional cloudiness, Sci., *245*, 1227-1230, https://doi.org/10.1126/science.245.4923.122 , 1989.

Ali, G., Bao, Y., Ullah, W., Ullah, S., Guan, Q., Liu, X., . . . Ma, J.: Spatiotemporal trends of aerosols over urban regions in Pakistan and their possible links to meteorological parameters, Atmo., 11, 306, https://doi.org/10.3390/atmos11030306, 2020.

Andreae, M., & Rosenfeld, D.: Aerosol–cloud–precipitation interactions. Part 1. The nature and sources of cloud-active aerosols, Earth. Sci. Rev., *89*, 13-41, https://doi.org/10.1016/j.earscirev.2008.03.001, 2008.

Anttila, T., Brus, D., Jaatinen, A., Hyvärinen, A. P., Kivekäs, N., Romakkaniemi, S., ... & Lihavainen, H.: Relationships between particles, cloud condensation nuclei and cloud droplet activation during the third Pallas Cloud Experiment, *Atmos. Chem. Phy.*, *12*, 11435-11450, https://doi.org/10.5194/acp-12-11435-2012 , 2012.

Anwar, K., Alam, K., Liu, Y., Huang, Z., Huang, J., & Liu, Y.: Analysis of aerosol cloud interactions with a consistent signal of meteorology and other influencing parameters, Atmos. Res., *275*, 106241, https://doi.org/10.1016/j.atmosres.2022.106241, 2022.

Brenguier, J.-L., Pawlowska, H., Schüller, L., Preusker, R., Fischer, J., & Fouquart, Y.: Radiative properties of boundary layer clouds: Droplet effective radius versus number concentration, Atmos. Sci., *57*, 803-821,https://doi.org/10.1175/1520-0469(2000)057<0803:RPOBLC>2.0.CO;2 , 2000.

Chen, F., Sheng, S., Bao, Z., Wen, H., Hua, L., Paul, N. J., & Fu, Y. : Precipitation Clouds Delineation Scheme in Tropical Cyclones and Its Validation Using Precipitation and Cloud Parameter Datasets from TRMM, Applied Met. Climatology. 57, 821-836,https://doi.org/10.1175/JAMC-D-17-0157.1 , 2018.

Chen, Q., Yin, Y., Jin, L.-j., Xiao, H., & Zhu, S.: The effect of aerosol layers on convective cloud microphysics and precipitation, Atmos. Res., *101*, 327-340, https://doi.org/10.1016/j.atmosres.2011.03.007, 2011

Costantino, L., & Bréon, F.: Analysis of aerosol-cloud interaction from multi-sensor satellite observations, Atmos. Sci., *37*,https://doi.org/10.1029/2009GL041828, 2010

Fan, C., Ding, M., Wu, P., & Fan, Y.: The Relationship between Precipitation and Aerosol: Evidence from Satellite Observation, Atmos. Oce. Phy.,https://doi.org/10.48550/arXiv.1812.02036, 2018.

Feingold, G., Eberhard, W. L., Veron, D. E., & Previdi, M.: First measurements of the Twomey indirect effect using ground-based remote sensors, Geophy. Res. Let., *30*, https://doi.org/10.1029/2002GL016633, 2003.

Gryspeerdt, E., Quaas, J., & Bellouin, N.: Constraining the aerosol influence on cloud fraction, *JGR.Atmos*,*121*, 3566-3583,https://doi.org/10.1002/2015JD023744 , 2016.

Hassan, M. A., Mehmood, T., Liu, J., Luo, X., Li, X., Tanveer, M., & Abid, M.: A review of particulate pollution over Himalaya region: Characteristics and salient factors contributing ambient PM pollution. Atmos. Envi., 294, 119472, https://doi.org/10.1016/j.atmosenv.2022.119472 , 2002.

Hong, Y., Hsu, K. L., Moradkhani, H., & Sorooshian, S.: Uncertainty quantification of satellite precipitation estimation and Monte Carlo assessment of the error propagation into hydrologic response, Wat. Resc. Res., 42, 8, https://doi.org/10.1029/2005WR004398 , 2006.

Hossain, F., Anagnostou, E. N., & Bagtzoglou, A.: On Latin Hypercube sampling for efficient uncertainty estimation of satellite rainfall observations in flood prediction, Comp. & geosc., 32, 6, 776-792, https://doi.org/10.1016/j.cageo.2005.10.006 , 2006.

Jiang, H., Feingold, G., & Cotton, W.: Simulations of aerosol-cloud-dynamical feedbacks resulting from entrainment of aerosol into the marine boundary layer during the Atlantic Stratocumulus Transition Experiment, JGR. Atmos., *107*, AAC 20-1-AAC 20-11, https://doi.org/10.1029/2001JD001502, 2002.

Jung, E.: Aerosol-cloud-precipitation interactions in the trade wind boundary layer, Ph.D Thesis, Meteorology and Physical Oceanography, University of Miami, 91-pp., 2012.

Kang, N., Kumar, K. R., Yin, Y., Diao, Y., Yu, X.: Correlation analysis between AOD and cloud parameters to study their relationship over China using MODIS data (2003-2013): impact on cloud formation and climate change,AAQR.,*15*, 958-973,https://doi.org/10.4209/aaqr.2014.08.0168 , 2015.

Kaskaoutis, D., Kumar Kharol, S., Sinha, P., Singh, R., Kambezidis, H., Rani Sharma, A.: Extremely large anthropogenic-aerosol contribution to total aerosol load over the Bay of Bengal during winter season, Atmos. Chem. Phy., *11*, 7097-7117, https://doi.org/10.5194/acp-11-7097-2011 , 2011.

Kedia, S., Ramachandran, S., Holben, B., & Tripathi, S.: Quantification of aerosol type, and sources of aerosols over the Indo-Gangetic Plain,Atmos.Envi.,, *98*, 607-619,https://doi.org/10.1016/j.atmosenv.2014.09.022, 2014.

Koike, M., Asano, N., Nakamura, H., Sakai, S., Nagao, T., & Nakajima, T.: Modulations of aerosol impacts on cloud microphysics induced by the warm Kuroshio Current under the East Asian winter monsoon, JGR. Atmos.,*121*,282-297,https://doi.org/10.1002/2016JD025375, 2016.

Kubar, T., Hartmann, D., & Wood, R.: Understanding the importance of microphysics and macrophysics for warm rain in marine low clouds. Part I: Satellite observations, Atmos. Sci. 66, 2953-2972, https://doi.org/10.1175/2009jas3071.1, 2009.

Kumar, A., & Physics, S.: Variability of aerosol optical depth and cloud parameters over North Eastern regions of India retrieved from MODIS satellite data,Atmos. Sol. Terr. Phy.,*100*, 34-49,https://doi.org/10.1016/j.jastp.2013.03.025, 2013.

Kump, L. R., & Pollard, D.: Amplification of Cretaceous Warmth by Biological Cloud Feedbacks, Sci., *320*, 195-195,https://doi.org/10.1126/science.1153883, 2008.

Li, J., Lv, Q., Zhang, M., Wang, T., Kawamoto, K., Chen, S., & Zhang, B.: Effects of atmospheric dynamics and aerosols on the fraction of supercooled water clouds, *Atmos. Chem. Phy.*, *17*, 1847-1863,https://doi.org/10.5194/acp-17-1847-2017, 2017.

López-Romero, J., Montávez, J., Jerez, S., Lorente-Plazas, R., Palacios-Peña, L., & Jiménez-Guerrero, P.: Precipitation response to aerosol–radiation and aerosol–cloud interactions in regional climate simulations over Europe. *Atmos. Chem. Phys., 21*, 415-430, https://doi.org/10.5194/acp-21-415-2021 , 2021.

Masmoudi, M., Chaabane, M., Tanré, D., Gouloup, P., Blarel, L., & Elleuch, F.: Spatial and temporal variability of aerosol: size distribution and optical properties, Atmos. Res., *66*, 1-19,https://doi.org/10.1016/S0169-8095(02)00174-6 , 2003.

McCoy, D., Field, P., Schmidt, A., Grosvenor, D., Bender, F., Shipway, B.,& Elsaesser, G.: Aerosol midlatitude cyclone indirect effects in observations and high-resolution simulations, *Atmos. Chem. Phy.*, *18*, 5821-5846, https://doi.org/10.5194/acp-18-5821-2018 , 2018.

Michibata, T., Kawamoto, K., & Takemura, T.: The effects of aerosols on water cloud microphysics and macrophysics based on satellite observations over East Asia and the North Pacific, Atmos. Chem. Phy., *14*, 10515-10541, https://doi.org/10.5194/acp-14-11935-2014 , 2014.

Myhre, G., Stordal, F., Johnsrud, M., Kaufman, Y., Rosenfeld, D., Storelvmo, T.: Aerosol-cloud interaction inferred from MODIS satellite data and global aerosol models, Atmos. Chem. Phy., *7*, 3081-3101, https://doi.org/10.5194/acp-7-3081-2007, 2007.

Nair, V., Giorgi, F., Keshav Hasyagar, U.: Amplification of South Asian haze by water vapour–aerosol interactions, Atmos,Chem.Phy., *20*, 14457-14471, https://doi.org/10.5194/acp-20-14457-2020 ,2020.

Naud, C., Posselt, D., & van den Heever, S.: Observed covariations of aerosol optical depth and cloud cover in extratropical cyclones, *JGR: Atmos*,*122*,10-338,https://doi.org/10.1002/2017JD027240 , 2017.

Rossow, W., & Schiffer, R.: Advances in understanding clouds from ISCCP, Bul. Americ. Meteor. Soci., *80*, 2261-2288, https://doi.org/10.1175/15200477(1999)080<2261:AIUCFI>2.0.CO;2 ,1999.

Sharma, P., Ganguly, D., Sharma, A., Kant, S., Mishra, S.: Assessing the aerosols, clouds and their relationship over the northern Bay of Bengal using a global climate model, Earth. Spac. Sci., *10*, e2022EA002706, https://doi.org/10.1029/2022EA002706, 2023.

Sherwood, S., Roca, R., Weckwerth, T., & Andronova, N.: Tropospheric water vapor, convection, and climate, Rev. of Geophy (AGU), 48, 2,https://doi.org/10.1029/2009RG000301, 2010.

Singh, A., Rastogi, N., Sharma, D., Singh, D.: Inter and intra-annual variability in aerosol characteristics over northwestern Indo-Gangetic Plain,AAQR., *15*, 376-386,https://doi.org/10.4209/aaqr.2014.04.0080, 2015.

Srivastava, P., Pal, D., Aruche, K., Wani, S., & Sahrawat, K.: Soils of the Indo-Gangetic Plains: a pedogenic response to landscape stability, climatic variability and anthropogenic activity during the Holocene, Earth. Sci. Rew., *140*, 54-71, https://doi.org/10.1016/j.earscirev.2014.10.010, 2015.

Stevens, B., & Feingold, G.: Untangling aerosol effects on clouds and precipitation in a buffered system, Nature, 461, 607-613,https://doi.org/10.1038/nature08281 , 2009.

Sun, J., & Ariya, P.: Atmospheric organic and bio-aerosols as cloud condensation nuclei (CCN): A review, Atmos. Envi., 40, 795-820,https://doi.org/10.1016/j.atmosenv.2005.05.052 , 2006.

Tao, W., Chen, J., Li, Z., Wang, C., & Zhang, C.: Impact of aerosols on convective clouds and precipitation, Rev. Geophys., *50*,https://doi.org/10.1029/2011RG000369, 2012.

739 Thomas, A., Kanawade, V., Sarangi, C., & Srivastava, A.: Effect of COVID-19 shutdown on aerosol direct
740   radiative forcing over the Indo-Gangetic Plain outflow region of the Bay of Bengal,Sci. Total Envi.,
741   *782*, 146918,https://doi.org/10.1016/j.scitotenv.2021.146918, 2021.
742 Tian, Y., & Peters-Lidard, C.: A global map of uncertainties in satellite-based precipitation
743   measurements, Geohys. Res. Let., 37, 24, https://doi.org/10.1029/2010GL046008 , 2010.
744 Tripathi, S. N., Pattnaik, A., & Dey, S.: Aerosol indirect effect over Indo-Gangetic plain, Atmos. Envi., 41, 33,
745   7037-7047, https://doi.org/10.1016/j.atmosenv.2007.05.007, 2007.
746 Twomey, S.: The influence of pollution on the shortwave albedo of clouds, Atmos. Sci., *34*, 1149-
747   1152,https://doi.org/10.1175/1520-0469(1977)034<1149:TIOPOT>2.0.CO;2 , 1977.
748 Verma, S., Ramana, M., & Kumar, R.: Atmospheric rivers fueling the intensification of fog and haze over Indo-
749   Gangetic Plains, Sci. Reports., Nature, *12*, 5139, 2022.
750 Wolf, E., & Toon, O.: Controls on the Archean climate system investigated with a global climate model,
751   Astrobiology, *14*, 241-253,https://doi.org/10.1089/ast.2013.1112, 2014.
752 Wood, R.: Relationships between optical depth, liquid water path, droplet concentration, and effective radius in
753   adiabatic layer cloud,University of Washington, *3*, 2006.
754 Wu, P., Dong, X., Xi, B., Liu, Y., Thieman, M., & Minnis, P.: Effects of environment forcing on marine
755   boundary layer cloud-drizzle processes, JGR: Atmos., *122*, 4463-
756   4478,https://doi.org/10.1002/2016JD026326, 2017.
757 Wyant, M., Bretherton, C., Bacmeister, J., Kiehl, J., Held, I., Zhao, M., Soden, B.: A comparison of low-latitude
758   cloud properties and their response to climate change in three AGCMs sorted into regimes using mid-
759   tropospheric vertical velocity, Clim. Dyn., *27*, 261-279, https://doi.org/10.1007/s00382-006-0138-4,
760   2006.
761 Yuan, T.: Increaseofclouddropletsizewith aerosolopticaldepth: Anobservationandmodelingstudy, JGR: Atmos.,
762   *113*, D4, https://doi.org/10.1029/2007JD008632, 2008.
763 *Yang, Y., Liu, X, Qu, Y., An, J., Jiang, R., Zhang, Y., & Ma, Q. : Characteristics and formation mechanism of*
764   *continuous hazes in China: a case study during the autumn of 2014 in the North China Plain. ACP., 15,*
765   *8165-8178,* https://doi.org/10.5194/acp-15-8165-2015, 2015.
766 Zeb, B., Alam, K., Sorooshian, A., Chishtie, F., Ahmad, I., Bibi, H.: Temporal characteristics of aerosol optical
767   properties over the glacier region of northern Pakistan, Jour. Atmos. Sol-Terr. Phy., *186*, 35-
768   46,https://doi.org/10.1016/j.jastp.2019.02.004, 2019.
769 Zhao, C., Tie, X., & Lin, Y.: A possible positive feedback of reduction of precipitation and increase in aerosols
770   over eastern central China, Geo. Res. Let., 33, 11, https://doi.org/10.1029/2006GL025959, 2006.
771 Zhou, S., Yang, J., Wang, W., Zhao, C., Gong, D., Shi, P.: An observational study of the effects of aerosols on
772   diurnal variation of heavy rainfall and associated clouds over Beijing–Tianjin–Hebei, Atmos. Chem.
773   Phy., *20*, 5211-5229,https://doi.org/10.5194/acp-20-5211-2020, 2020.

774